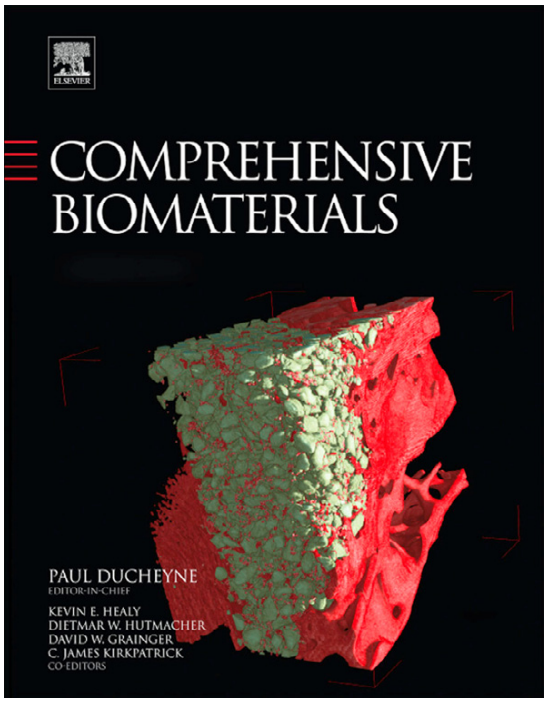

Ting L.H. and Sniadecki N.J. (2011) Biological Microelectromechanical Systems (BioMEMS) Devices. In: P. Ducheyne, K.E. Healy, D.W. Hutmacher, D.W. Grainger, C.J. Kirkpatrick (eds.) Comprehensive Biomaterials, vol. 3, pp. 257-276 Elsevier.

3.315. Biological Microelectromechanical Systems (BioMEMS) Devices

L H Ting and N J Sniadecki, University of Washington, Seattle, WA, USA

Glossary

Actin A protein present in all eukaryotic cells that compromises the cytoskeleton of a cell. Actin monomers polymerize together to form a double helical strand known as a microfilament or thin filament. The pointed end of actin has slower rate of adding new actin monomers to the strand than the barbed end.

Adherens junction Cadherin and catenin protein complexes at the cell membrane that serve as intracellular attachments linking neighboring cell cytoskeletons together. Traction forces can be transmitted from one cell actin structure through an adherens junction to a cell in contact.

Extracellular matrix Network of complex macromolecules that form a scaffold that cells adhere to. Common structural extracellular matrix proteins are collagen and elastin and common adhesive proteins are fibronectin and laminin.

Focal adhesion Large protein assemblies at the cell membrane that anchor a cell to the extracellular matrix through integrin receptors. Focal adhesion formation is a GTPase-dependent process and serves to transmit forces between the extracellular matrix and the cell's cytoskeleton.

Focal adhesion kinase (FAK) A tyrosine kinase present at focal adhesions that promotes turnover of cell contacts with the extracellular matrix.

Microcontact printing Protein transfer technique akin to a stamp and ink procedure that is used to control available binding sites for biomolecules or cells. A soft elastomer stamp has a protein absorbed to it and is put in contact with the target surface transferring the protein pattern over.

Myosin Motor proteins that interact with actin filaments for motile processes within a cell. Many isoforms exist, with myosin I and myosin II being the most frequently referred to. Myosin I has a single head binding domain and an ATP independent actin-binding site. Myosin II comprises two heavy chain ATPase domain heads and four light chain tails. With ATP present, heavy chains alternate attachment to an actin filament and walk along the filament to generate force.

Rho A GTPase protein encoded by the Rho genes that regulates actin dynamics. Downstream protein signal regulators include Dia1 and the ROCK subfamily. Their broad range of action affects cell adhesion, gene expression, motility, and proliferation.

Comprehensive Biomaterials (2011), vol. 3, pp. 257-276

Soft lithography Replication of a surface or topography by applying a liquid elastomer onto a surface, curing it, and then peeling the surfaces apart to form a negative mold. Repeating this procedure with the negative mold reproduces the original features.

Traction force The force exerted by a cell through its actin–myosin contractile apparatus that allows it to migrate. Traction forces are transmitted through the focal adhesions of a cell.

Abbreviations

AFM	Atomic force microscopy
BioMEMS	Biological microelectromechanical systems
DEP	Dielectrophoresis
ECM	Extracellular matrix
ELISA	Enzyme-linked immunosorbent assay
F-actin	Filamental actin
FAK	Focal adhesion kinase
G-actin	Globular actin
GAG	Glycosaminoglycan
GFP	Green fluorescent protein
GTPase	Guanosine triphosphatase
MEMS	Microelectromechanical systems
MTC	Magnetic twisting cytometry
PDMS	Polydimethylsiloxane
ROCK	Rho kinase
UV	Ultraviolet

3.315.1. Introduction

Cells respond to biochemical and biomechanical stimuli through changes in their proliferation, apoptosis, differentiation, secretion, contraction, motility, and adhesion. To better understand these changes in cellular behavior, researchers have developed biological microelectromechanical systems (BioMEMS) that provide a high degree of control over the stimuli that cells receive from their surroundings. Cells are cultured commonly on dishes, which are not only stiffer and flatter than a cell's native tissue, but they also lack the appropriate chemical and mechanical signals that cells experience *in vivo*. The techniques and processes from BioMEMS can provide a means to control a wide variety of microenvironmental cues in order to better understand the nature of the cellular response.[1,2] Findings that have come from the use of BioMEMS have influenced the design of biomaterials and tissue-engineered constructs because engineers and scientists can begin to incorporate the appropriate interactions for cells.

Cells in living tissue have different levels of cues than their counterparts in culture. The vascular and lymphatic systems provide cells with the appropriate nutrients and hormones for their survival and function. Likewise, the levels of oxygen and growth factors in culture can be excessive for cells and overdrive their response. These chemical interactions influence cell behavior by engaging surface receptors that activate specific signal pathways. Gradients in signal molecules can also serve to attract cells to locations or activate particular responses. In addition to these soluble factors, the insoluble cues that a cell encounters from its extracellular matrix (ECM) are different than those in tissue. Tissue culture dishes are coated usually with one kind of ECM protein such as collagen or fibronectin or reconstituted extracts such as Matrigel, whose contents are poorly defined. These insoluble factors are not well-matched to the different variety of adhesive ligands that a cell type may require. Moreover, cells experience a variety of extracellular forces from their surroundings that act on the mechanosensory structures in a cell that influence its behavior.[3,4] These forces come from the range of physiological phenomena such as pressure forces from muscle contraction, shear forces from vascular hemodynamics, traction forces from surrounding cells, or stretching forces from musculoskeletal locomotion. Emerging evidence shows that biomechanical factors such as substrate stiffness and cell geometry can influence cell functions such as migration,[5] cytokinesis,[6] differentiation,[7,8] and growth.[9,10] These findings are important because they implicate that cells in one kind of environment respond differently than those in another. Since the influence of different factors must be careful examined, robust means to explore these factors are required.

BioMEMS has provided important insights in improving the development of biomaterials or tissue-constructs to better represent the cellular microenvironment, either by closely matching the native one or specifically activating a cellular response. Many of these tools are derived from microelectromechanical systems (MEMS) such as actuators or posts but have been adapted by researchers interested in probing cells at the nanoscale. BioMEMS devices can be used to measure traction forces that cells produce against a surface, which is important to maintain stable adhesion against a substrate. These tools can also be incorporated with techniques to impart forces onto the surface of a cell to examine the mechanotransduction response. Cell culture and microfluidics can be combined to create chemical gradients or shearing forces that cells experience *in vivo*. In all these cases, BioMEMS provides a powerful way to manipulate physical forces and chemical factors that interact with a cell to better understand the role of a cell's microenvironment.

3.315.2. Cell Adhesions to the Microenvironment

Cells in living organisms bind and adhere to a network of ECM proteins. This meshwork of protein provides the structural scaffold necessary for cells to form stable adhesions (**Figure 1**). ECM proteins include collagen, elastin, laminin,

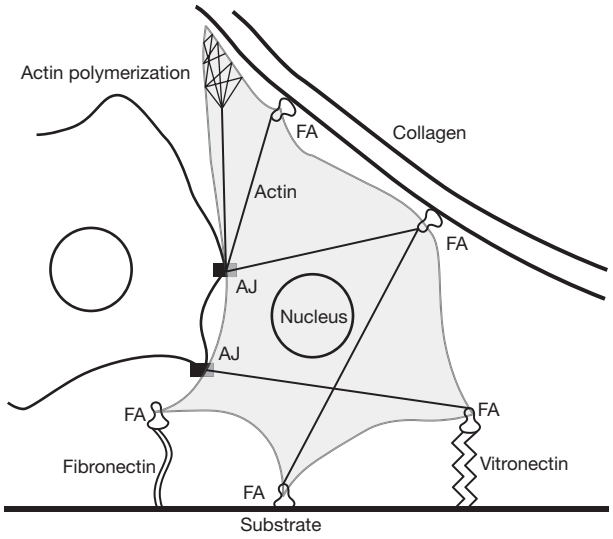

Figure 1 Cells adhere to the extracellular matrix through focal adhesion (FA) sites that connect intracellularly to the actin cytoskeleton. Neighboring cells connect their cytoskeletons at adherens junctions (AJ). A cell changes its shape in order to spread or migrate by polymerizing its actin filaments so that they can push against the cell membrane.

fibronectin, vitronectin, and many other proteins to varying degrees of concentration and spatial organization. The main function of the ECM is to provide cells with ligands for the binding of their integrin receptors, which are not only essential for cell adhesion but also activate signaling pathways that affect cell function.[11] Integrins also coordinate activities within a cell's cytoskeleton, such as actin filament polymerization and focal adhesion assembly, which are important in stabilizing the adhesion of a cell against a substrate.[12,13]

When an integrin receptor contacts a ligand site on an ECM protein, signal pathways associated with RhoGTPases Rho and Rac are activated. In eukaryotic cells, there is an abundant quantity of the monomeric, globular actin (G-actin) within the cell. Rho and Rac can activate actin-binding proteins that cause G-actins to bind to each other to create filamental actin (F-actin).[14] F-actin elongation occurs as more G-actins become recruited to the growing filament, but with the pointed end growing faster than the barbed end. F-actin growth can be prevented by capping proteins that inhibit the addition of G-actin at the free ends, severing proteins that cleave the filament at points along its length, or depolymerizing proteins that promote the dissociation of G-actin from the ends.[15] This dynamic remodeling of actin allows the filaments to push the cellular membrane forward during spreading, a critical component of cell survival[9] and migration. It also provides the freedom for the cell to adapt its structure to response to its surroundings.

When myosin and α-actinin bind to F-actin, the structure is called a stress fiber and has the ability to shorten its length to create tension inside the cell. Myosin acts to slide two or more F-actin filaments past one another so that the cell can contract.[16] A cell then produces traction forces by transmitting its cytoskeletal tension from actin and myosin to its focal adhesions where integrins are clustered together and firmly bound to ligands in the ECM. The major signaling pathway for stress fiber regulation is Rho and its downstream effectors Rho kinase (ROCK or ROK) and mDia1.[14] The dual action of ROCK directly phosphorylates myosin light chain and inhibits myosin light chain phosphatase. The Rho effector mDia1 serves as a nucleating agent at the cell membrane for new actin polymerization.[17]

Focal adhesions are not static structures, but respond to ligand binding and applied forces. They are large, multiprotein complexes that structurally connect the actin cytoskeleton to the ECM and can activate signaling networks that are essential for morphogenesis, migration, proliferation, differentiation, and survival.[18] Focal adhesions form at the cytoplasmic side of the cell membrane after integrins bind to the ECM. Focal adhesion proteins such as talin, vinculin, and paxillin colocalize with integrins and help to improve the bond strength of the adhesion site by gathering many integrins within a close proximity and also by mechanically coupling the integrins to the actin.[13] Interestingly, cytoskeletal tension from actin and myosin is needed to promote the growth of focal adhesions, indicating that these structures have a mechanotransduction response to force. Focal adhesions also serve as docking sites for signaling proteins such as focal adhesion kinase (FAK) and Src that regulate tyrosine phosphorylation pathways and guanine–nucleotide exchange factors (GEFs) and GTPase-activating proteins (GAPs) that regulate Rho GTPases.[18] Specifically, an important balance exists between pathways associated with Rho and FAK, which serve to encourage adhesion reinforcement or disassembly. Rho activity increases focal adhesion formation,[19] but FAK can act to suppress Rho and therefore promote detachment of focal adhesions during cell motility.[20]

The compliance in ECM proteins gives some insight into how cells interact with their microenvironment. At the molecular level, ECM proteins are surprisingly stiff materials. Collagen, for example, has an elastic modulus of around 5 GPa,[21] but as a reconstituted gel, it is significantly softer. Comparatively, bone is between 10 and 20 GPa and soft tissue is between 10 and 100 kPa,[22,23] so there is a significant range of stiffness that cells can experience in their native environment. Common engineered materials used in biological applications such as titanium alloy and stainless steel are 114 and 190 GPa, respectively[24] and many plastics, including polystyrene which is used in tissue culture dishes, have an elastic modulus between 2 and 4 GPa. Thus, it is important to be aware that in designing biomaterials and tissue-constructs that their material properties need to be matched to the native tissue so as to illicit the appropriate mechanotransduction effect on the cells.

The compliance of the ECM has been shown to play a role in the dynamic binding of a cell's integrins. Certain ECM proteins such as fibronectin can be unraveled under tension to reveal new ligand sites on which a cell can bind.[25] These 'cryptic' sites become available under force and are therefore hypothesized to be regulated by traction forces of a cell or external forces from physiological motion.[26] Cells have also been observed to bind differently to synthetic matrices that are highly compliant. On polyacrylamide gels, cells show changes in their spreading and motility that depended on the environmental stiffness (**Figure 2**).[27] Focal adhesion structures are also noticeably reduced on softer gels and have lower kinase activity as compared to cells on stiffer gels or plastic tissue culture dishes. This suggests that ECM stiffness increases focal adhesion formation in addition to cytoskeletal tension. In fact,

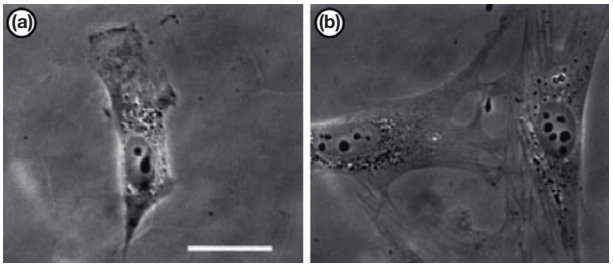

Figure 2 (a) Cell on a soft substrate spreads less than (b) cells on a stiff substrate. Scale bar is 10 μm. Reproduced from Pelham, R. J., Jr.; Wang, Y. *Proc. Natl. Acad. Sci. USA* **1997**, *94*, 13661–13665 with permission, Copyright 1997 National Academy of Sciences, USA.

gradients in stiffness can also affect the direction of cell migration as cells have been observed to move toward stiff regions and away from softer regions.[5]

Much of the native interaction that cells have with their microenvironment is lost with traditional cell culture. Common procedures seed cells onto polystyrene dishes or flasks and grow the cells in an incubator to maintain correct temperatures and pH levels. Polystyrene dishes are convenient, cost-effective, and well-established surfaces on which to culture and observe cells. Manufacturing standards have made it possible for dishes from different suppliers to elicit the same cell attachments and behaviors while remaining inert to cells and chemicals. Polystyrene is certainly the most widely used surface to culture and experiment with cells, offering high optical clarity and visibility, and complete compatible with phase light, fluorescent, and confocal microscopy techniques, but it is also a more rigid environment than cells experience *in vivo*.

By departing from traditional culture approaches, it has been possible to observe how cells regulate their function in response to the stiffness of their environment. Cardiomyocytes improve their contractile performance when plated onto gels that match the stiffness of the native myocardium.[28] Stem cells are able to commit to a neurogenic lineage on soft gels and osteogenic lineages on stiff gels based on their ability to generate cytoskeletal tension.[7] A three-dimensional matrix environment also affects cells for they show reduced levels of cytoskeletal and focal adhesion activities as compared with cells on ECM-coated substrates.[29] Thus, there needs to be a better understanding on the biochemical and biomechanical factors that drives these changes in cell adhesions and BioMEMS can provide important insights for the design of biomaterials and tissue-constructs. For additional information, see **Chapter 4.403, The Innate Response to Biomaterials**.

3.315.3. BioMEMS Devices to Measure Traction Forces

Cell force measurement tools arose in response to observations that cells in culture were motile and so it was likely that they were imparting forces to move. It was suspected that they produced traction forces against the surface of the culture dish, but techniques were limited in measuring these nanoscale forces. The advent of MEMS fabrication techniques provided a means to create tools and sensors that matched the size of the cell. Researchers adopted these techniques to create new tools that followed a common macroscale approach to measure force: direct contact with a flexible, calibrated structure and observation of its deflection under a load. Sensor structures such as these can be fabricated and designed to measure a wide range of physiological cell forces, such as single cell contraction and multicellular interactions.

3.315.3.1. Membrane Wrinkling

A pioneering development that laid the groundwork for future BioMEMS devices was Albert Harris' work in 1980. He and his colleagues observed that cells exerted traction forces by culturing cells on a deformable, silicone membrane substrate.[30] To make the surface, a layer of silicone fluid, polydimethylsiloxane (PDMS), was spread out on a glass coverslip. Flame was then used to cross-link the top layer of the silicone to create a thin, elastic film on top of the remaining liquid silicone film, which acted as a support and lubricant for deflection. Cells placed on this film distorted the top surface and caused wrinkles that were due to the tangential forces they exerted from actin and myosin contraction (**Figure 3(a)**).[31,32] By correlating the membrane wrinkle length with a magnitude of force, the technique was later able to provide a closer measure of the traction forces, but the approach was still semiquantitative.[33] An important finding from Harris' pioneering work was that fibroblast forces were far larger than what is needed for locomotion, in fact two or three magnitudes more. This led to the theory that these strong forces are necessary for the physical remodeling of the ECM.[34] When fibroblasts were seeded onto collagen gels, they observed that the traction forces of the cells pulled the gel into a dense capsule of collagen fibers similar to the formation of wrinkles in the silicone films. They theorized that the traction fields created by the cells can form the aligned collagen fiber structures seen in tissues such as tendons or ligament, rather than relying on an existing matrix to induce the alignment.

A limitation of PDMS wrinkling films is that there is low resolution in measuring traction forces because there exists a mechanical coupling between a wrinkle in a substrate and the traction forces nearby. A traction force is applied at a single focal adhesion of a cell, but the surface strains in the film leads to wrinkling over a wider area. The overlap in strains from nearby traction forces makes it difficult to determine how much each one contributes to a visible wrinkle in the film. The elasticity of the silicone film also means that the traction forces of a cell can cause a strain in the film over a widespread area, which can subject neighboring cells to an external stretch or wrinkled surface topology. Quantifying wrinkles is also a vague approach because it is difficult to interpret what is and what is not a wrinkle due to debris or surface defects in the silicone film.

Refinements were made to the silicone wrinkling technique by using surface markers that enabled a higher resolution and a better understanding of the deformations caused by traction forces. Marker beads were placed on top of the PDMS film to track displacement of the film over a high number of spatial points. To create this substrate, one micrometer diameter latex beads were deposited onto the PDMS fluid and its top surface was cross-linked in a glow discharge chamber.[35] An improved mathematical and statistical model for the deformation of the film used the tracking of the beads, rather than wrinkles.[36] Additionally, the

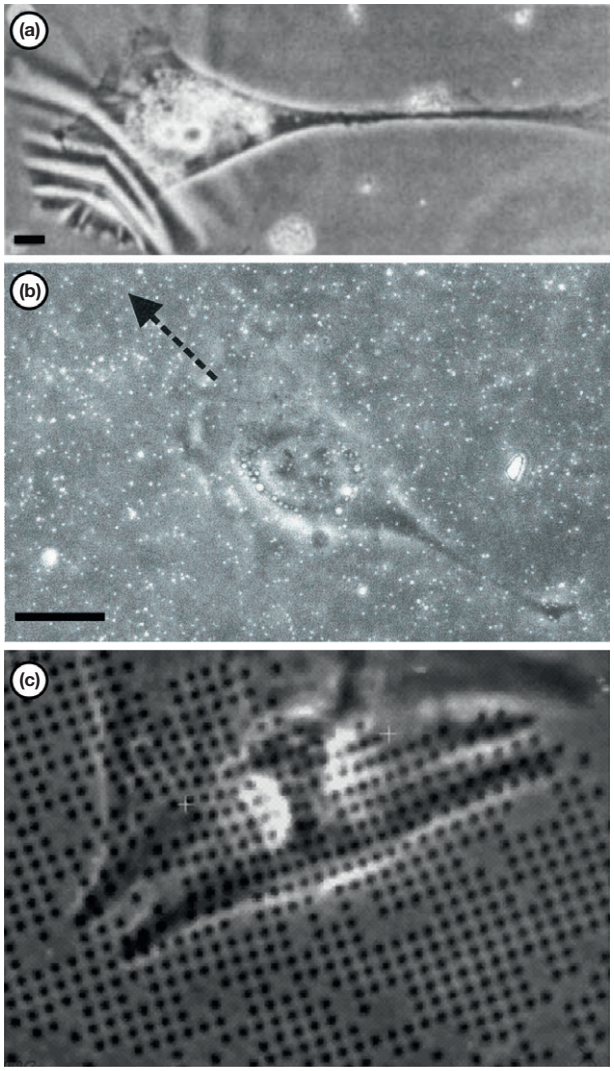

Figure 3 (a) Cell wrinkling of a silicone membrane floating on silicone fluid. Force is orthogonal to the long axis of each wrinkle and the stretch of the traction force correlates with the length of the wrinkles. Scale bar is 10 μm. (b) Traction force microscopy technique with cell on polyacrylamide gel containing embedded fluorescent beads, which act as fiduciary markers of strain at the surface of the substrate. Scale bar is 20 μm. (c) BioMEMS traction force microscopy where marker dots are patterned into a 2-μm grid pitch. Some dots are missing from the fabrication process, but surface strains are evident by the displacements of the markers from their original positions as evenly spaced rows and columns. Adapted from Harris, A. K.; Stopak, D.; Wild, P. *Nature* **1981**, *290*, 249–251; Munevar, S.; Wang, Y.; Dembo, M. *Biophys. J.* **2001**, *80*, 1744–1757; Balaban, N. Q.; Schwarz, U. S.; Riveline, D.; *et al. Nat. Cell Biol.* **2001**, *3*, 466–472.

approach allowed for an order of magnitude improvement in detectable forces compared to wrinkling membranes.

3.315.3.2. Traction Force Microscopy

A popular method to measure subcellular level forces is traction force microscopy which measures traction forces by the distortion of cells on polyacrylamide gels instead of on PDMS films.[37] The gel is mixed with fluorescent beads that are a few micrometers or smaller in diameter and spread out as a thin film on a glass coverslip on which cells can be cultured (Figure 3(b)). To engage integrins to bind and promote cell adhesion, an ECM protein such as collagen or fibronectin can be coated onto the surface of the gel. The completed fabrication process results in a deformable gel on which cells can be cultured and whose embedded fluorescent particles can be tracked to measure cellular traction forces. Cells seeded into this environment adhere to the ECM protein, form focal adhesions and actin stress fibers, and exert cytoskeletal traction forces onto the substrate. The deformation of the gel pulls with it the fluorescent particles. Their positions can be recorded under fluorescence microscopy and compared to the original, undeflected positions of the particles to obtain the deflection field. Calculation of a traction force field from a measured deflection field in an elastic material is known as a Boussinesq problem in the field of mechanics and can be readily solved. Traction force microscopy has been used to show that the forces of a cell increase with stiffness of a substrate, adhesive ligand density, and contact area.[5,38,39] Normal and transformed cells also exhibit distinct patterns of traction forces across the leading and tail edges when migrating with normal cells having organized zones of forces and transformed cells displaying weak disorganized mechanical domains.[40]

Patterns of traceable markers can be generated for traction force microscopy by using a microfabricated stamp from a silicon wafer that has arrays of dot-like features (Figure 3(c)).[41] The stamp can be used to deposit fluorescent material onto the surface of a PDMS substrate to create a uniform array of marker dots. Cells deform the surface, and traction forces can be measured with more accuracy due to the regularity of the pattern as opposed to the random placement of beads in polyacrylamide gels. One disadvantage of traction force microscopy is that it shares the same problem as silicon wrinkling films in that the gels or PDMS is a continuous material and so the solution for the traction forces is difficult to obtain without a degree of uncertainty.

3.315.3.3. MEMS Adapted Tools

MEMS techniques and devices have played a key role in developing an understanding of traction forces. Atomic force microscopy (AFM) was one of the first tools used to reveal cellular properties. Extreme sensitivity and miniscule local sampling area on the order of 0.01 μm^2 means that researchers can use it to sample very localized responses.[42] AFM takes measurements by lowering a nanometer scale tip onto the surface of interest. A piezoelectric sensor detects cantilever deflection and can also impart simple or cyclic deflections to the tip giving a way to impart force as well. The AFM technique opened the field to direct force measurements of properties of whole cells,[43] cell cytoskeletons,[44] subcellular organelles, and biomolecules.[45]

A novel approach is the fabrication of a set of horizontal cantilevers that have micrometer-scale dimensions (Figure 4).[46] Micromachining is used to create the cantilever, which is a manufacturing process where thin layers of polysilicon, silicon dioxide, and metals are deposited onto a wafer and then each layer is selective etched to create a final structure. The horizontal cantilever is built underneath the surface of the device but

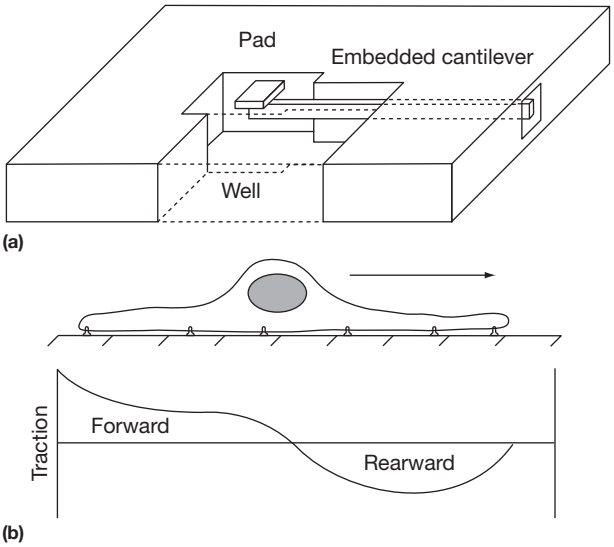

Figure 4 (a) BioMEMS traction force device with embedded, horizontal cantilever inside a well. A migrating cell can attach to the pad at the opening of the well and deflect the cantilever under its traction force. (b) Traction forces of a migrating cell measured with the device show pulling forces at the leading edge and pushing forces at the tail. Reproduced from Galbraith, C. G.; Sheetz, M. P. *Proc. Natl. Acad. Sci. USA* **1997**, *94*, 9114–9118 with permission. Copyright 1997 National Academy of Sciences, USA.

surrounded by a well that was etched to allow the cantilever to freely deflect. A pad is attached at the free end of a cantilever to allow the cell to bind and is used to mark the displacement of the cantilever tip. Cells placed onto this device can adhere and spread on the top surface. As a cell migrates, it comes in contact with a cantilever's pad and forms a focal adhesion. The traction force produced by actin and myosin causes the cantilever to bend. The deflection of the cantilever is readily visible under optical microscopy, which then allows the calculation of traction forces during migration. The use of BioMEMS cantilevers showed that the magnitude of traction forces differs across regions of the cell during migration. As the cell proceeds in one direction, the leading edge creates contractile forces toward the nucleus, increasing this traction force in the region behind the lamellipodia. These traction forces reverse in the rear of the cell, indicating the cell is pushing against the substrate to propel itself. Fibroblast cells move by continuous generation of focal adhesions at the front and release of adhesions at the rear, again through the influence of actin and myosin. The measurement of traction forces by a single cantilever, however, prevents simultaneous force measurement across all regions of the cell as seen with traction force microscopy. The force that is measured can only be determined on an axis perpendicular to the length of the cantilever, so the true strength and direction of the force are not directly resolved.

3.315.3.4. Microposts

Soft lithography can be used to create arrays of vertically aligned PDMS cantilevers, which are referred to as microposts.[47] To form the master, a thick film of photoresist is patterned on a silicon wafer using photolithography to create arrays of microposts that are up to tens of micrometers in height and a few micrometers in diameter (Figure 5(a)). Fluorosilane is applied during this process to act as a nonadhesive release layer. Uncured PDMS is poured on top of the microposts features of the master and subsequently cured by heat to create a negative mold with 'microholes.' The negative mold then can be used to replicate the micropost features of the master. PDMS is poured on top of the mold, cured, and then peeled off to create the arrays of PDMS microposts used for cell culture. The elastic stiffness of the posts can be controlled by the physical dimensions of diameter and height of the microposts giving the sensors multicellular capabilities with different cell types.

PDMS is a useful material for BioMEMS researchers due to its high biocompatibility, surface chemistry, and ease of use and fabrication. Favorable mechanical properties include predictable elastomeric properties, thermal stability, gas permeability for cell culture purposes, and optical transparency in imaging and observation.[48] PDMS can be sterilized through several means: immersion in 70% ethanol, UV exposure, or autoclaving.[49] It also has a hydrophobic surface that can be useful in certain applications, but it can also be modified with plasma oxidation to render it temporarily hydrophilic.[50] In microcontact printing, changing the hydrophobicity of PDMS is useful in order to allow proteins to transfer from a hydrophobic PDMS stamp onto a hydrophilic PDMS substrate.[51] In microfluidics, a temporarily hydrophilic surface is desirable to enhance the wetting of the fluid into small channels. Plasma oxidation of PDMS also allows it to covalently bond to other polymers and glass. Ozone treatment can produce a similar result as plasma oxidation, but is significantly slower and does not weaken the PDMS structure.[48] Silane is a common surface treatment for PDMS because it reacts with available hydroxyl groups on the surface to form covalently bonded Si–O–Si molecules on the surface. A wide variety of silanes are available that can be used to create new functional groups on the PDMS surface.[48,52] In replica molding of the PDMS micropost array, the negative molds are treated with fluorosilane in order to ensure easy peeling of the arrays from the mold.

Biofunctionalization of the micropost array is achieved by patterning ECM proteins onto the top surface of the micropost tips. A PDMS stamp with the appropriate pattern is molded from an SU-8 or a silicon structure (Figure 5(b)). ECM proteins in solution are deposited onto the surface of the PDMS stamp and then the stamp is used to print a pattern of ECM onto the tips of the micropost array (Figure 5(c)). Subsequent treatment with Pluronics can be used to prevent cell adhesion at any surface of the microposts that has not been stamped with ECM protein. Pluronics is a nonionic copolymer consisting of ethylene oxide and propylene oxide, whose amphiphilic nature makes it a powerful surfactant. It adheres to the unstamped regions of PDMS to form a single-molecule thick coating that prevents other molecules from adsorbing to the surface. Thus, cells are confined to form focal adhesions to only the stamped tips of the posts (Figure 6(a)).

In order to measure strength of the traction forces on the posts, it is important to accurately track the displacement of the tips.[53,54] Originally, the displacements were identified by immunofluorescently staining the ECM at the tips of the posts.[47] A common treatment now is to submerge the micropost arrays in DiI solution, which is a hydrophobic dye which

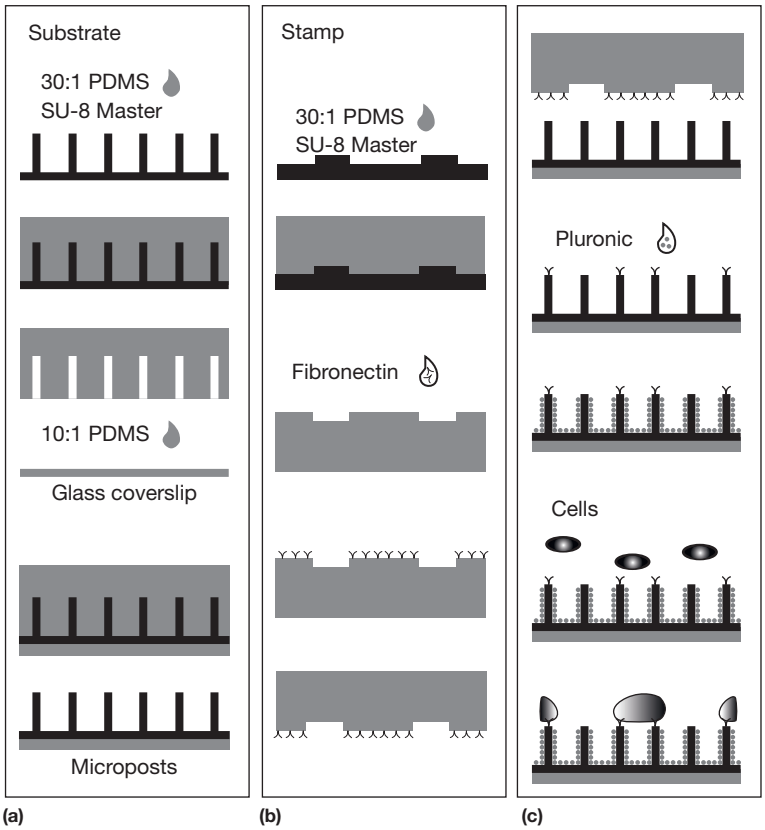

Figure 5 Micropost fabrication technique. (a) A master is created using photolithography of SU-8 or silicon (not shown) and then double-cast in PDMS to produce arrays of micropost. (b) For microcontact printing, stamps are created to pattern ECM proteins on the surface of the posts. (c) After stamping, Pluronic is used to block the adsorption of proteins onto unstamped surfaces in order to control cell adhesion.

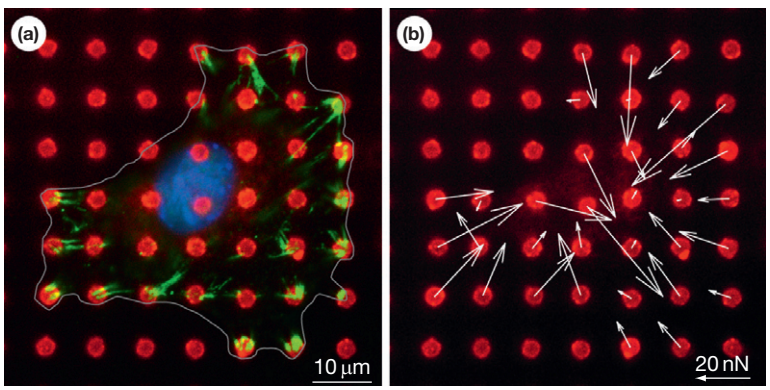

Figure 6 (a) A cell spreads across the tips of multiple microposts and forms focal adhesions. (b) Fluorescent labeling of the posts allows for traction force measurements as force vectors. Scale bar is 10 μm and scale arrow is 20 nN. Adapted from Sniadecki, N. J.; Anguelouch, A.; Yang, M. T.; *et al*. *Proc. Natl. Acad. Sci. USA* **2007**, *104*, 14553–14558.

labels the PDMS in the infrared spectrum. Microposts can also be marked by depositing quantum dots in the tips of the posts[55] or by phase contrast microscopy.[56,57] A local traction force is determined from the post's deflection δ and is given by $F = 3\pi E D^4 \delta / 64 L^3$, where E is the elastic modulus of PDMS, D is the diameter, and L is the length of the post. Microposts have been made with diameters between 2 and 5 μm and lengths between 5 and 15 μm. From these measurements, it is possible to determine the traction force field that cells exert on the microposts (Figure 6(b)). By adjusting the dimensions of the microposts, it is possible to tailor the stiffness of the array to look at how cells adjust their traction forces in response to matrix compliance[58] or anisotropic material properties.[59]

Microposts are a useful tool for examining individual cells, but the idea can be extended to larger and smaller scales as well. Micropost flexibility can be adjusted by increasing the dimensions to measure the high forces generated by cardiac myocytes (Figure 7(a)).[60] Large microposts ('megaposts') have been

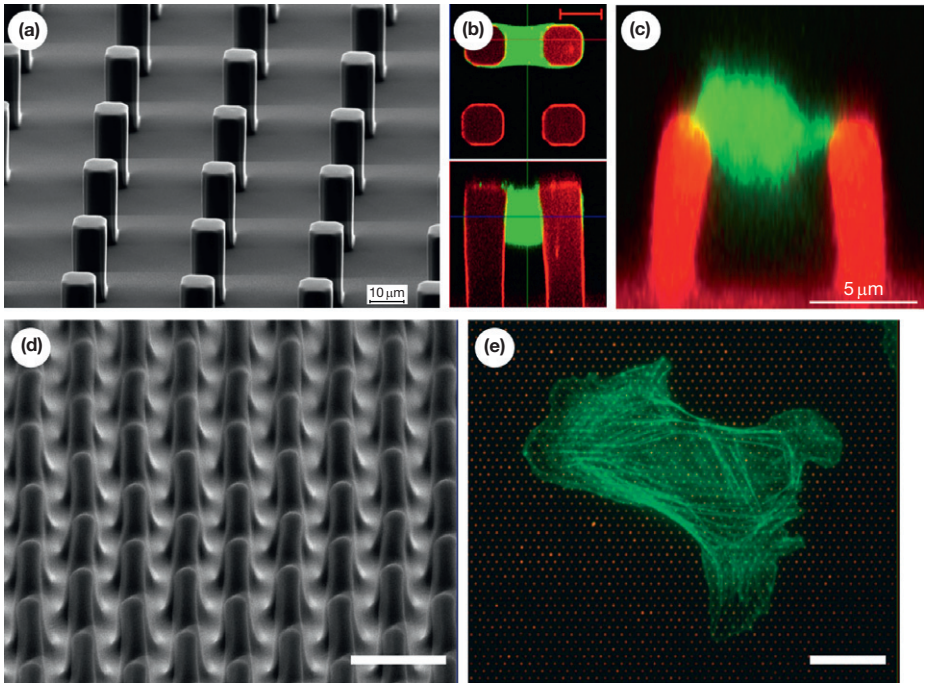

Figure 7 (a) Scanning electron microscope (SEM) image of megaposts. (b) Actin-labeled cardiac myocyte suspended between two megaposts. Scale bar is 10 μm. (c) Platelet microclot suspended between a pair of microposts. (d) SEM image of nanoposts. Scale bar is 10 μm. (e) Cell spread on nanoposts and have more defined cytoskeletal structures. Scale bar is 10 μm. Adapted from Kajzar, A.; Cesa, C. M.; Kirchgessner, N.; Hoffmann, B.; Merkel, R. *Biophys. J.* **2008**, *94*, 1854–1866; Liang, X. M.; Han, S. J.; Reems, J. A.; Gao, D.; Sniadecki, N. J. *Lab Chip* **2010**, *10*, 991–998; Yang, M. T.; Sniadecki, N. J.; Chen, C. S. *Adv. Mater.* **2007**, *19*, 3119.

used to test single cardiac myocytes that have been isolated to adhere to pairs of large posts (Figure 7(b)). Observation shows periodic myocyte contraction rates and large force ranges of 140–400 nN, which is beyond the measurable range with other techniques. The megapost approach has also been used to measure tissue-construct forces that arise from the combination of cells and ECM into a microtissue.[61] The samples are made by seeding cells and collagen into molds that were hundreds of microns long and containing two megaposts at either end. As the cells gather with collagen, they pull on the megaposts revealing bulk dynamics. In an approach similar to megaposts, pairs of microposts were used to measure the contractile forces that platelets generate when they aggregate together to form a clot and then retract (Figure 7(c)).[62] Recent developments have reduced the dimensions of the microposts to create nanoposts (Figure 7(d)).[63] These smaller dimensions allow for a significantly higher packing density of posts underneath a cell that creates a quasismooth surface on which a cell can spread (Figure 7(e)). The cytoskeletons in cells on the nanoposts closely resemble those observed for cells on flat surfaces. The reduced spacing also allows cells or cellular structures to be analyzed that are too small to fit between individual microposts. As the technology to fabricate BioMEMS improves, it is likely that the adhesive and physical interactions between smaller cells and subcellular structures will be more deeply explored.

Unlike the deformation of continuous films or gels, individual microposts are independent sensors because the deflection at one post does not affect the measurement of force at another post. Thus, these arrays lend themselves to measuring a large field of forces from multiple cells and different configurations of patterning can be done to test a wide gamut of multicellular interactions. Cells in a monolayer form adherens junctions with neighboring cells, and microposts have been used to examine the mechanical interactions in sheets of cells.[56,64] Bowtie patterns can also be used so that the tugging force between pairs of cells can be measured in isolation (Figure 8(a)).[65] Fibronectin was patterned onto the microposts to confine the contact between two cells. Since the pair of cells is connected through their adherens junctions, the vector sum of traction forces of one of the cells is not zero, but is in fact the tugging force from the neighbor cell. It was found cells that had a greater length of adherens junction with each other were able to support a higher tugging force. It was found that Rho mediated the tugging force and the Rac regulated the increased adherens junction assembly length. This mechanical interplay between cells shows that with groups of cells on the microposts, maximum forces are at the edge of the monolayer and exceed those of a single cell, indicating that collective mechanical signaling may be occurring.[56] This signaling can lead to a mechanotransduction response because cells at the edges or corners of a monolayer had higher traction stresses against the ECM due to the tugging forces of their neighbors, and this stress caused increased proliferation of cells at the edge (Figure 8(b)).[64] Heterogeneous cell–cell interactions can also promote higher traction forces because individual endothelial cells within a monolayer exerted higher forces on the microposts when they were in contact with a transmigrating monocyte (Figure 8(c)).[66]

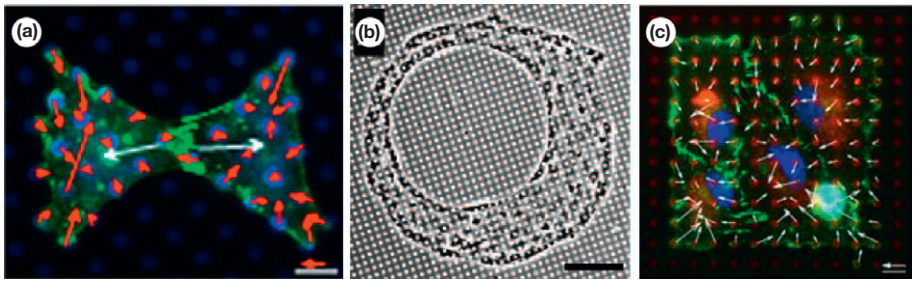

Figure 8 (a) Cells patterned to bowties on microposts can be used to measure the tugging force at adherens junctions. Scale bar is 10 μm, scale arrow is 10 nN. (b) Endothelial cells patterned into an eccentric circle shape on the microposts. Scale bar is 100 μm. (c) Monocyte transmigration through endothelial cells can be measured on microposts. Scale bar is 10 μm, scale arrow is 32 nN. Adapted from Liu, Z.; Tan, J. L.; Cohen, D. M.; *et al*. *Proc. Natl. Acad. Sci. USA* **2010**, *107*, 9944–9949; Nelson, C. M.; Jean, R. P.; Tan, J. L.; *et al*. *Proc. Natl. Acad. Sci. USA* **2005**, *102*, 11594–11599; Liu, Z. J.; Sniadecki, N. J.; Chen, C. S. *Cell. Mol. Bioeng.* **2010**, *3*, 50–59.

3.315.4. BioMEMS Devices to Apply Forces to Cells

Cells sense forces and modulate their cytoskeleton and regulatory proteins accordingly.[67] The three main cytoskeletal filaments actin, intermediate filaments, and microtubules transmit forces within a cell, and can become linked to neighboring cells cytoskeleton through transmembrane junction proteins such as at adherens junctions. Cells therefore relay forces to cells around them, as well as experience forces acting on them from their microenvironment. The importance of these transmitted forces in tissue is important in the development of the cardiovascular, musculoskeletal, and nervous systems, all of which have been shown to be influenced by mechanical forces.[68]

Arterial remodeling provides an interesting example of cellular mechanotransduction. Arteries are mechanically compliant, and when blood is driven through them, they expand elastically with each pressure wave from the cardiac cycle. The distensible nature of the arterial tissue acts as a stretchable substrate on which endothelial cells adhere. Strains up to 10% are normal for arterial tissue, and these strains can be recreated *in vitro* by culturing cells on flexible PDMS membranes that are stretched uniaxially. Cells have been observed to change their shape and realign their actin cytoskeletons in a direction perpendicular to the applied strain. However, when Rho activity is inhibited, these cells align in a direction parallel to the stretching, suggesting that external force is sufficient to induce actin remodeling.[69]

Mechanotransduction has been hypothesized to occur at a variety of cellular structures, but the cytoskeleton has been strongly implicated to have a central role since it connects to the focal adhesions and adherens junctions. When cells on a PDMS membrane were treated with a detergent to keep the cytoskeletons intact but strip away the lipid membranes and cytoplasmic proteins, it was found that cytoskeletons that were stretched had significantly higher amounts of focal adhesion proteins.[70] This response is similar to the growth response at the focal adhesion due to traction forces.[41] Additionally, the protein response at the focal adhesion suggests that mechanotransduction occurs from conformation changes.[71] Force may cause unfolding of focal adhesion proteins to reveal new domains for the binding of adaptor or signaling proteins or it may also expose enzymatic domains that then activate signaling activity associated with mechanotransduction. For additional information, see **Chapter 5.527, Cardiovascular Tissue Engineering**.

3.315.4.1. Micromanipulation

Tests with large strains and stresses are useful for simulating tissue level dynamics but single cell systems are of equal interest. Cellular responses to a localized force can be useful in examining a mechanosensor in a cell. The most direct approach is to use micromanipulation techniques with a glass pipette.[72] To form this tool, a pipette is heated until its melting temperatures and then pulled into a long, sharp tip before being allowed to cool. Because the tip diameter can be as small as 1 μm, its deflection can be used to measure the amount of force applied to the cells. These tool tips can be biofunctionalized by coating with an ECM protein such as fibronectin to ensure that integrins adhere to the tip and form focal adhesions. It has been observed that applied force can create growth at focal adhesions near the tip. It has also been shown that the externally applied mechanical stress can bypass the need for ROCK-mediated cytoskeletal tension in order to cause the growth of focal adhesions.

AFM has been used to impart forces to biological materials,[73] but larger forces and more degrees of freedom in positioning the manipulator may be of interest. MEMs micromachining can produce probing tools for applying localized cell forces with wider force ranges than AFM and with greater accuracy than glass micropipette techniques. A micromachined device consisting of suspended, flexible beams has been created from silicon wafers (**Figure 9(a)**).[74] A probe tip on a translatable backbone beam is connected to pairs of flexible beams that are fixed to the base silicon structure. As the probe tip is pushed against a cell, the change in lateral distance between the tip and a fixed reference point can be used to indicate the force (**Figure 9(b)**). Applying pulling force to axons has shown that tension causes vesicles that contain neurotransmitters to accumulate at the presynaptic terminal, indicating that neuromuscular synapses use tensile forces in regulating synaptic function (**Figure 9(c)**).[75]

3.315.4.2. Magnetic Bead Forces

A technique for applying forces is magnetic twisting cytometry (MTC).[76] Here, a ferromagnetic microbead is coated with an Arg-Gly-Asp (RGD) peptide sequence, which is a ligand for integrins. These beads can then be bound to the surface of a cell and mechanical stress applied by rotating the beads through a magnetic field (**Figure 10**). Probing individual

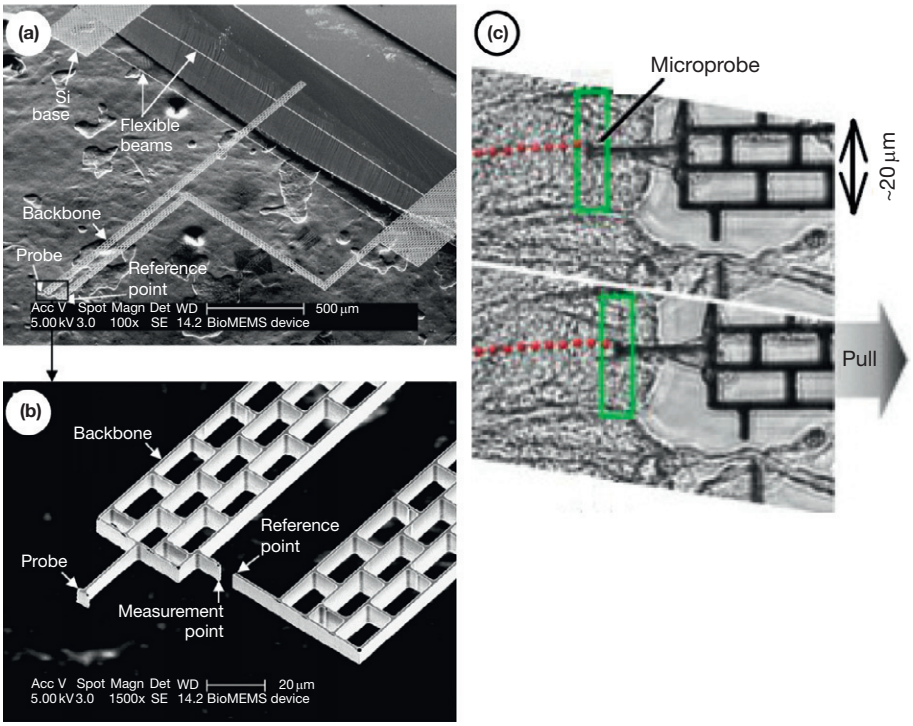

Figure 9 (a) Suspended BioMEMS manipulator structure made from silicon. (b) Force measurement is conducted by monitoring the distance between the probe and reference point on a fixed beam. (c) Force from the manipulator can be used to examine mechanotransduction in nervous tissue. Adapted from Yang, S.; Saif, T. *Rev. Sci. Instrum.* **2005**, *76*; Siechen, S.; Yang, S. Y.; Chiba, A.; Saif, T. *Proc. Natl. Acad. Sci. USA* **2009**, *106*, 12611–12616.

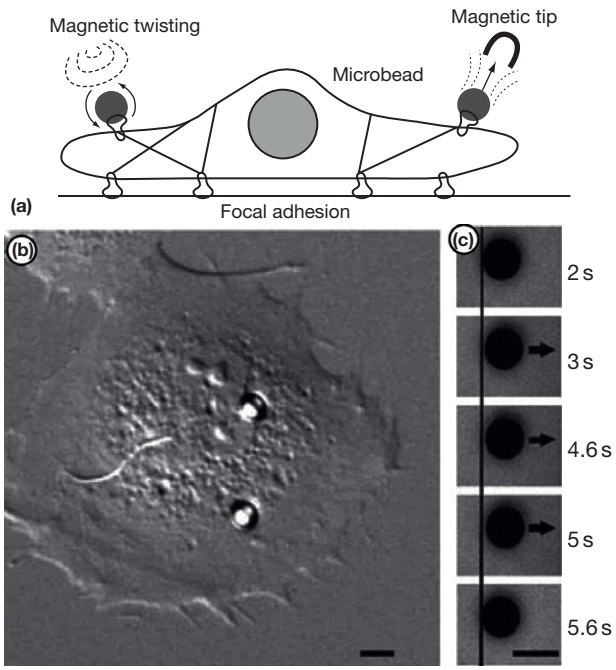

Figure 10 (a) Magnetic microbeads bound to integrins on a cell are rotated by a uniform magnetic field or pulled into the gradient of a magnetic field emanating from magnetic tip. (b) Two microbeads attached on a cell's surface are pulled on and (c) the response shows a displacement starting at time of 3 s and ending after 5 s. Scale bars are 5 μm. Adapted from Matthews, B. D.; Overby, D. R.; Alenghat, F. J.; *et al. Biochem. Biophys. Res. Commun.* **2004**, *313*, 758–764, with permission from Elsevier.

focal adhesions through MTC demonstrated that a cell stiffens its mechanical attachment to the bead to prevent it from twisting. A similar response was observed with magnetic tweezers, where an integrin-bound magnetic bead is pulled into the gradient of a magnetic field.[77] Early reinforcement depends on the structural integrity of the cytoskeleton, but the active strengthening of the adhesion site to a sustained force from the bead requires Rho, ROCK, Src, and stretch-activated ion channels.[78] Combining MTC with fluorescence resonance energy transfer gives a way to visually observe the activation of proteins under applied loads.[79] In particular, Src has been observed to become activated at both the local focal adhesion where force is applied and at remote sites. The rate of activation at the remote sites is 50 times faster than what is possible through soluble factor-induced signaling and can be inhibited by pharmacologically disrupting microtubule and actin filaments to prevent the transmission of force along the cytoskeleton.[79,80] Thus, mechanical forces acting through the cytoskeleton might be a rapid and efficient signaling cue to inform cells about their microenvironment as opposed to diffusive, soluble signals. It has been revealed by using MTC that mechanotransduction signals can also propagate across adjacent cells through their adherens junctions.[81] Interestingly, vinculin, which is a protein that is associated with both the focal adhesion and with the adherens junctions, has been observed to accumulate at the E-cadherin adhesion complex under applied force.[82] Since cell–cell adhesions appear to have a similar mechanotransduction response as cell–ECM adhesions, the cytoskeleton likely plays an integral role in directing these mechanical forces to the appropriate mechanosensory structures.[83]

3.315.4.3. Optical Traps/Tweezers

Optical traps are another method that can measure and induce forces at the subcellular level. The technique uses a focused laser to produce a force on a dielectric microbead, which can be embedded at the surface or in the cytoplasm of a cell. Beads can be used to apply forces to focal adhesions, but non-ECM proteins can be coated onto the beads to probe a variety of biophysical interactions within a cell. As long as the bead's dielectric material has a higher refractive index than the surrounding medium, when the bead is in focal point of the beam, it experiences an optical force toward the center of the beam. This restoring force is due to change in momentum of the photons from refraction as the laser light passes through the bead. If the center of the beam is moved, the bead will experience a stronger restoring force that moves it toward the position of the laser's focal point. The distance of the bead from the center of the focal point is a close approximation to the strength of the restoring force and is usually measured using a photodiode.

Optical tweezers have been used to show that focal adhesion strengthening occurs with applied force.[84] Vinculin is observed to accumulate at the site of applied force using beads coated with only the cell-binding domains of fibronectin.[85] The accumulation of the focal adhesion proteins likely involves the early binding of talin to the fibronectin-integrin complex that provide initial strength to the adhesion site.[86] The applied force also activates Src, which regulates the growth of the integrin–cytoskeleton connection.[87] The stiffness at the cellular membrane can also be examined with optical tweezers, where an isoform of myosin, myosin-1a, has been found to be essential in linking the membrane to the underlying cortical cytoskeleton.[88]

Larger field effects for applying forces to cells can also be created. An optical method, known as optical stretching, uses two lasers that face one another (**Figure 11(a)**).[89] A cell trapped between the two lasers is trapped at the focal point, but also experiences a gradient of forces from the refracted beams that cause a stretch to its entire volume (**Figure 12(b)–12(d)**). This technique functions as long the refractive index of the cell is higher than the surrounding fluid environment. The stretching force that can be generated by the gradients is significantly larger than for two beads pulling with optical tweezers. Also the use of divergent beams produces less risk of radiation damage to the biomolecule or cell. An important consideration for optical stretching is that it is limited to the study of nonadhesive cells as many cells will undergo apoptosis without adequate integrin engagement.

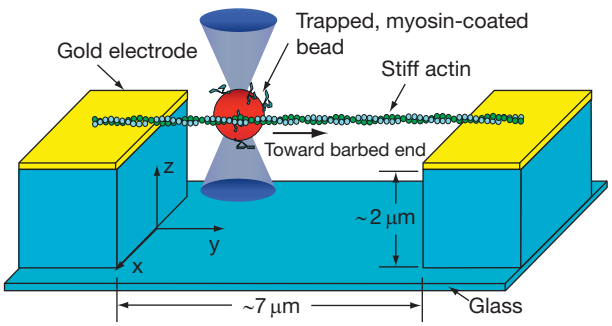

Figure 11 Myosin coated bead placed with optical tweezers migrating on an actin filament, which is held in tension between two gold adhesion pads. Adapted from Arsenault, M. E.; Sun, Y.; Bau, H. H.; Goldman, Y. E. *Phys. Chem. Chem. Phys.* **2009**, *11*, 4834–4839, with permission from Royal Society of Chemistry.

Optical techniques provide high sensitivity at the nanoscale and can be used to measure single biomolecule mechanics.[90] To do so, a bead is attached to one end of a molecule with the other end anchored to a nonmoving surface. It is possible to examine the stretch response in a molecule under an applied load by moving the optical trap away from the anchored molecule and observing the bead's change in distance from the trap's focal point. Sensitivity is so high that in fact optical traps are limited only by environmental noise from the substrate, since it is theoretically possible to resolve angstrom scale length changes. To address the noise, a second optical trap and microbead can replace the anchored point on a biomolecule, enabling even finer forces to be measured.[91] Not only does it provide a way to study how force can change the structure of a protein or biomolecule such as DNA, it also provides a measure of strain recovery times, spring constants, and internal molecular coefficients of friction, thus providing a richer mechanical analysis of single molecules.[90]

In particular, the mechanical interactions between actin and myosin can be examined to better understand how this fundamental process underlies the mechanics of cells. Optical tweezers have been used to determine that myosin bound to a nonmoving surface can produce 3 pN of force on average with each power stroke against a single actin filament that is held in an optical trap.[92] Improvements to this approach have demonstrated that actin filaments can be aligned across a gap between two gold electrode by using an AC field (**Figure 12**).[93] Tension in the filament is controlled by the electric field which allows a straight actin filament to be formed between the gold electrodes. A bead coated with myosin V or myosin X is brought in contact with the actin filament and released from the optical tweezer. Interestingly, the path that the bead took under myosin's motor action was helical as it traversed toward the barbed end of the filament. A similar helical path has been seen for myosin II,[94] suggesting that the motor action of myosin involves a degree of torque as it progresses along the length of actin.

3.315.4.4. Magnetic Microposts

A recent development in BioMEMS has been the use of PDMS micropost arrays with embedded magnetic nanowires. Magnetic cobalt nanowires are manufactured through electrochemical deposition into a sacrificial alumina template with 300 nm diameter pores. Once released from the template, the nanowires are suspended in ethanol and then aliquoted onto the PDMS negative mold under a magnetic field, which pulls the nanowires down into the wells that form the microposts. Once the ethanol is evaporated away, PDMS is then poured into the negative mold to form the micropost arrays. The PDMS encapsulates the nanowires that are deposited into the wells, and once the PDMS array is peeled from the mold, the nanowires are found to be embedded inside individual posts, which are referred to as magnetic posts (**Figure 13(a)**).[95] Biofunctionalization of the microposts is performed using the

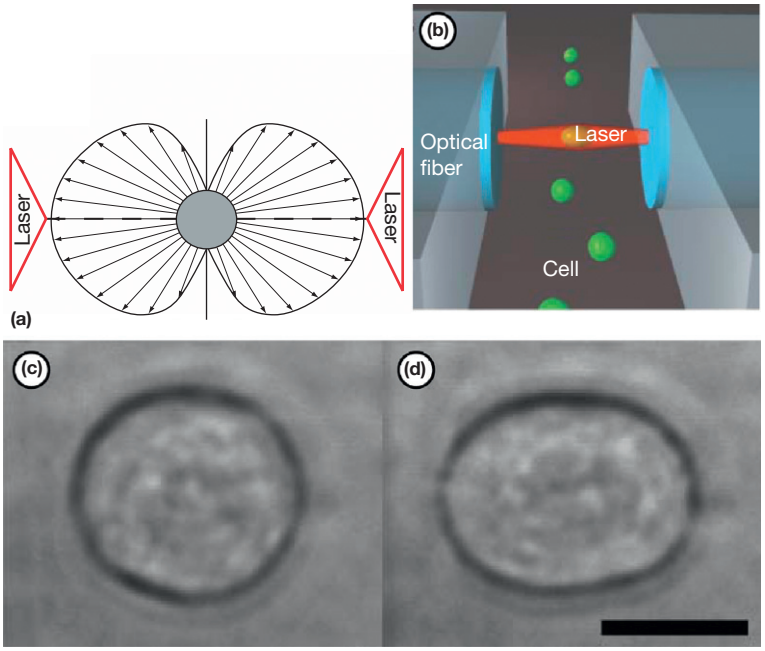

Figure 12 (a) Divergent focusing of two optical tweezers results in whole-cell stretching forces. (b) Combining the optical stretcher within a microfluidic channel allows for high-throughput trapping and stretching of a cell. (c) Phase light images of a trapped cell without stretch and (d) under optical stretch. Scale bar is 10 μm. Adapted from Guck, J.; Schinkinger, S.; Lincoln, B.; *et al. Biophys. J.* **2005**, *88*, 3689–3698, with permission from Elsevier.

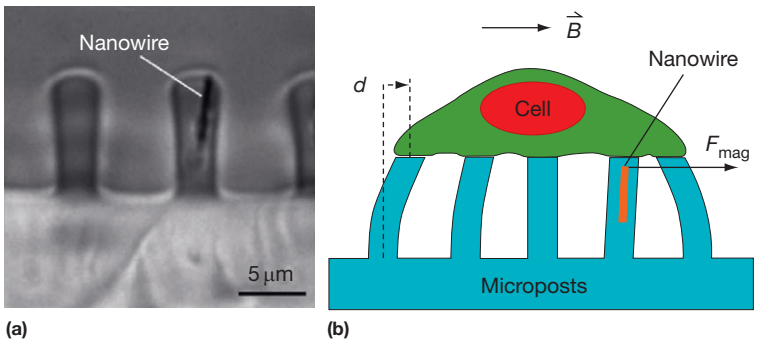

Figure 13 (a) Phase image of micropost cross section with embedded cobalt nanowire. (b) External force can be imparted to a cell at the magnetic post by applying a magnetic field, while traction forces can be measured at the nearby nonmagnetic posts. Adapted from Sniadecki, N. J.; Anguelouch, A.; Yang, M. T.; *et al. Proc. Natl. Acad. Sci. USA* **2007**, *104*, 14553–14558.

same techniques as with nonmagnetic micropost arrays. When a cell is seeded onto the surface of the microposts, they adhere at the tips and form focal adhesions and stress fibers just as if they were on flat substrates. PDMS posts that have the magnetic nanowires are able to be actuated when a horizontally applied uniform magnetic field is presented (**Figure 13(b)**). Deflection of a magnetic post introduces a controlled stress to the basal contact surface of the cell that induces growth at the local focal adhesion. Since a cell spreads onto multiple posts, its traction forces can be measured through the surrounding nonmagnetic posts. The posts are mechanically isolated from each other, so force actuation at a magnetic post does not impact the measuring ability at its neighbors. This has the advantage of being able to exert clearly measurable directionality and magnitude of force without worrying about force contributions from neighboring regions. The use of magnetic microposts has revealed that a cell responsds to an applied force at one or more of its focal adhesions with a rapid loss in cytoskeletal tension that slowly recovers after the stimulation.[54] This suggests that a cell can adjust its cytoskeletal structure in response to mechanical cues in its microenvironment.

3.315.4.5. Cytoskeletal Force Response

Under stretch from a silicone membrane, a cell's cytoskeleton tends to quickly fluidize before recovering and solidifying over time.[96] Under the solid-like state, biochemical interactions within a cell are highly specific, where the stable structures of the cytoskeleton are formed from distinct ligand-binding site interactions. Upon stretching a cell, it experiences a

structural transition into a chaotic, glassy-like phase where nonspecific interactions from proteins released from the disrupted cytoskeleton cause a crowded, molecular environment. Specifically, the stretching stimulus acts as a kind of 'enzymatic trigger' that causes the actin cytoskeleton to rapidly depolymerize. As a cell's structure turns over into a glassy-like state, there is a transitional drop in its stiffness. Newly freed G-actin monomers then polymerize into F-actin to resolidify the cell and cause its stiffness to return to prestretch levels. Treating cells with F-actin stabilizer jasplakinolide and applying stretch shows that the cell has a larger decrease in stiffness, but also recovers quickly to its pretreatment stiffness. Recent research has also examined fluidization and recovery in response to stretch using traction microscopy tools. Cells placed on polyacrylamide gels with isotropic or anisotropic stretches have traction forces that rapidly decrease after stretch which then recovers over time. These responses are seen in other diverse cells such as smooth muscle, endothelial, and osteocytes.[97]

3.315.4.6. Nanoscissors

The structural recovery of actin can be observed directly by snipping actin stress fibers inside a cell using a highly focused, femtosecond laser. Actin filaments in cells expressing GFP-actin can be targeted for ablation without causing large spread heating effects to the cell.[98,99] Cutting actin with a laser causes the filaments to instantaneously pull apart and continue to retract over many seconds. This is interpreted as the release of elastic tension in the strand, as well as gives insight to the viscoelasticity of the filaments and the fluid resistance of the cytoplasm.[98] Combining nanoscissor with traction force microscopy gives researchers the ability to measure the force contributions of single stress fibers. Severing a single fiber revealed a progressive loss in cytoskeletal tension for a cell. For cells on stiff substrates, cutting a fiber with the laser resulted in very minor cell elongation. On soft substrates, however, the severed stress fiber caused significantly higher cell elongation. Traction force mapping showed that the focal adhesion linked to the severed stress fiber displaced outward from the cell, furthering the evidence that cytoskeletal tensions are responsible for cell morphology and adhesion stability. The viscoelastic relaxation seen for cutting a single fiber is distinct from the rapid relaxation for cells stretched on silicone membranes or pulled on with magnetic posts. It is likely that local severing of actin causes a slow response because the remaining cytoskeletal structure is intact while the other techniques stimulate focal adhesion signals that cause massive disruption to the cytoskeleton's structural integrity.

3.315.5. Microfluidic Systems

BioMEMS provides tools that give better control over the microenvironment of the cell and, in particular, can be employed to present a myriad of mechanical and chemical factors to the cells. Constant or varied fluidic shear can be applied across single or multiple cells. Other factors that cells would see in their native environment such as stretch or pressure responses may be added. The microscale approach lends itself to the analysis of single cells in a high-throughput manner, which can be useful in filtering out heterogeneous responses within a subpopulation of the cells.[100] Moreover, more than one cell type may be cocultured together in a microfluidic system to gauge responses to released soluble factors and transmembrane signaling at their cell–cell contacts.

An added benefit of microfluidics is the high degree of control over waste product removal and nutrient addition. Typical protocols require that one changes a culture's nutrient media every 48 h.[101] Common growth factors such as serum become depleted in these intermittent times, while proliferating cells produce increasing amounts of undesirable waste products. Compared to static cell cultures, microfluidic systems and bioreactors typically have large volumes of media which translates to a volumetric buffer that minimizes chemical profile changes over time. The motion of the media also continuously refreshes the local media at the cell level, maintaining a steady amount of available biomolecules. Compared to static culture, cells in microfluidics can be confined to far narrower bands of available growth factor or signaler molecule concentrations.

3.315.5.1. Fluid Shear Stress

In many biological systems, mechanical shear stress from fluid flow plays a vital role in regulating cell morphology and function. These effects can be seen in flow systems as diverse as cardiovascular blood flow and interstitial cell flow. It has been well documented that the structure and physiology of the vasculature is heavily influenced by shear rate and flow type.[4,102] Vascular cells are exposed to a wide variety of flow conditions ranging from highly turbulent flows in the heart and major arteries to extremely laminar flows in arterioles and venules.

Mechanotransduction response by endothelial cells is of particular interest because of its close relation to atherosclerosis development. In normal function, the endothelium acts as a nonadhesive and nonclotting layer that protects arterial tissue from developing fatty lipids and invasive leukocytes in the intima. When the endothelium is damaged by shear, its barrier function deteriorates and lipids and macrophages are found to be in abundance in the artery wall. Once there, cytokines released from the affected area recruit additional leukocytes to the site where they accumulate lipids and swell the artery wall. Vascular smooth muscle cells proliferate within the damaged region and contribute to wall thickening by further releasing growth factors, chemoattractants, and vascular cell adhesion molecule.[103]

Initial damage can be caused by direct injury or endothelial cell remodeling in response to below average shear or disturbed shear regimes with high shear gradients. Endothelial cells express an atheroprone gene profile when exposed to these flow conditions.[104] However, laminar shear stresses cause a conformal remodeling of individual cells to reinforce their barrier function by promoting cell–cell junctions.[105] As mentioned previously, cells can align in response to applied stretch. However, different cells have different mechanotransduction responses. Mouse 3T3 fibroblasts align parallel to the applied strain, while endothelials align perpendicular.[69] Specific response also exists in shear stress as endothelial cells align parallel, but vascular smooth muscle cells align perpendicularly.[106] Endothelial cell realignment under fluidic shear has

also been confirmed with AFM examination of the surface topology.[107] Results show that shear-aligned cells display distinct surface ridges comprised of cytoskeletal actin. Non-sheared cells have smooth surfaces devoid of these features.

Platelets are another blood cell type that respond to mechanical shear. Decelerating hemodynamic shear microgradient profiles can activate platelets and cause thrombus formation.[108] Microfluidic experimentation has been a way to reveal this behavior. Other studies have shown that a critical rate of shear and exposure exists that, once passed, initiates activation regardless of shear conditions afterward. This can present problems downstream in the vasculature.[109] Platelet formation from megakaryocytes can be examined using BioMEMS apparatuses as well. Megakaryocytes are grown in a layered chamber separated by a porous membrane. Shear forces are applied to the system by gentle agitation. The megakaryocytes are seen to extend proplatelet-like protrusions through the membrane with an observation that agitated cells break off fragments of themselves.[110]

In examining the cellular response to shear, it is critical to know the flow conditions that a cell experiences *in vivo*, as well as the flows that are produced within a bioreactor or microfluidic device. Computer simulation of actual arteries utilizes magnetic resonance imaging or ultrasound scanning to generate a contoured interior surface of vessels for fluid flow simulations.[111] Direct methods exist for characterizing the flow inside a microchannel or flow chamber. Microscale particle image velocimetry is a technique that can be used to visualize and measure patterns in the flow field.[112] Here, microbeads or other tracer particles are added to a fluid and as they are carried along with the fluid, they report the local direction and velocity of the flow. These techniques are helpful in calibrating the flow conditions applied to cells.

3.315.5.2. BioMEMS Reactors

BioMEMS microfluidic devices are frequently used to apply moving fluid to cells. To do so, a channel is formed with biocompatible materials and functionalized. Channel shape, dimensions, and flow rates are all parameters that can be adjusted to control the flow dynamics. A proven and well documented method of channel fabrication is through PDMS replication molding of channels on a silicon wafer created through surface micromachining or photolithography techniques.[50] Complex geometries can be fabricated with this method, and valves and multiple flow conditions can be incorporated into one device. The material used to fabricate the device is flexible in many cases. For most applications, glass is the desired material due to its optical clarity, robustness, nonporous nature, and resistance to all sterilization techniques. However, machining glass and maintaining optical clarity and surface smoothness is a difficult task. Other common biocompatible replacement materials are acrylic, polystyrene, and polycarbonate. These offer similar optical transparency, can still be sterilized, and are easy to reconfigure in a laboratory setting. Plasma treatment of glass or a polymer creates a highly adhesive surface that forms a watertight seal with PDMS and is employed in many bioreactor designs.[48] For live-cell observation, a glass coverslip makes an ideal bottom surface of a bioreactor due to its thinness, a requirement for high magnification microscope objectives.

Cells are introduced to microfluidic systems by suspending them in media and injecting media through the microchannel. The cells settle and adhere to the surface and washing steps remove unattached cells. Since the vascular wall is comprised of more than endothelial cells, researchers have examined the effects of coculture on alignment and adhesion.[113] First, a layer of smooth muscle cells is seeded onto a substrate and grown to quiescent confluence. Next, endothelial cells can be directly seeded on top of the first layer and allowed to proliferate to confluence. The result is a bilayer of cells that closely resembles the endothelium in structure. The two cell types are able to form transmembrane gap junctions for chemical signaling, as well as respond to mechanical stresses through adherens junctions.

3.315.5.3. Bioreactor Pumping

To create fluid flow, different pumping schemes are used to achieve the desired flow in the microchannels. In the most basic flow device, pressure produced either through a raised fluid reservoir or gas source can drive fluid through a microfluidic system while a pump cycles the fluid back into the reservoir source. However, the lack of feedback-control means that researchers require more precise means. Syringe pumps provide excellent control if low flow rates are needed, but with limited volumes. Configuring multiple syringes and valves together can create a unidirectional flow that can recirculate to maintain the supply volume. Large flow rates use a peristaltic pump, also known as a roller pump, to have precise control of the flow. Peristaltic pumps produce a nonsteady pressure to the flow, which can be desirable if researchers want pulsatile flow. In most cases, a steady flow rate is desired, so air dampeners are placed in the fluid path to remove the effect of the pulses.[114] For additional information on other types of fluid flow devices, see **Chapter 5.511, Rotating-Wall Vessels for Cell Culture**.

3.315.5.4. Bioreactor Configuration

In BioMEMS microfluidic applications, ducts are the most common channel shape because shear is well defined and can be controlled precisely by dimensional considerations (**Figure 14(a, 1–8)**). Certain assumptions about the length-to-width aspect ratio mean that the wall shear stresses in the microchannels can be approximated to shear stress in parallel-plate flow. Shear forces at the wall can be calculated using: $\tau = 6\,\mu Q/WH^2$, where τ is shear stress, μ is viscosity, Q is fluid volumetric flow rate, W is the width, and H is the height of the channel. With steady pumping schemes, a constant level of shear stress gradient is produced at the wall surface. Adding a weir or obstruction in the channel initiates a disturbance in the flow that causes recirculation or vorticity at a region downstream. Between the weir and the vorticity reattachment point, a range of shear stresses and shear stress gradient exists.

Research has been done to determine the role of shear on endothelial cell morphogenesis. Endothelial cells placed into a duct with weir configuration display alignment characteristics that depend on their location in the channel. In steady, positive-direction laminar shear or steady, negative-direction laminar shear, the cells align parallel to the direction of flow.

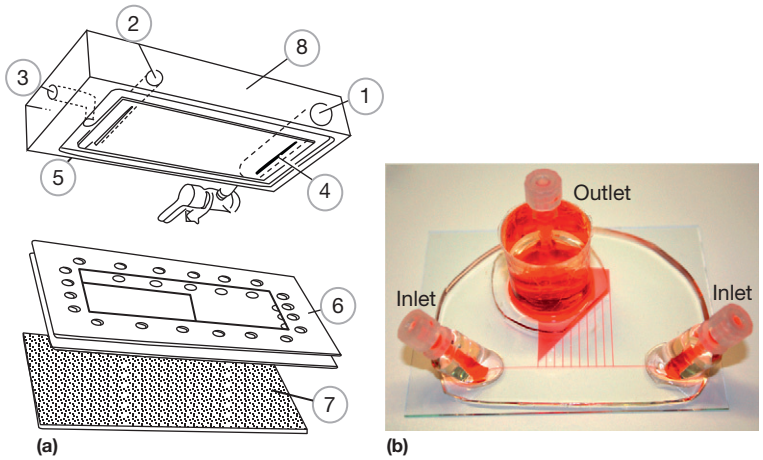

Figure 14 (a) Fluidic shear chamber utilizing parallel-plate channels. Fluid enters at (1), runs into the channel at slit (4), out of the channel (5), and leaves the device at (2). A gasket (6) seals a glass cover slide (7) with the polycarbonate top plate (8). Vacuum pressure through the (3) perimeter channel forms a seal for the device. (b) BioMEMS can be used to create multiple fluidic shears that are applied simultaneously to a common culture of cells by using differing channel lengths. The device is fabricated from replica molding of PDMS and treated with plasma to bond it to an underlying glass slide. Adapted from Chiu, J. J.; Wang, D. L.; Chien, S.; Skalak, R.; Usami, S. *J. Biomech. Eng.* **1998**, *120*, 2–8; Chau, L.; Doran, M.; Cooper-White, J. *Lab Chip* **2009**, *9*, 1897–1902.

Cells in regions with vorticity and below average shear stress have visible gaps between the cells, indicating a breakdown in their protective barrier function. Immunofluorescent imaging for F-actin filaments and microtubules additionally shows cytoskeletal fibers align in the direction of steady laminar flow and with no distinct alignment for low shear.[115]

A BioMEMS device fabricated with multiple channels of different lengths produces shear stress over a range of different magnitudes to the same culture of cells (**Figure 14(b)**).[116] The advantage here is that a single passage of cells can be used in the experiment and scarce samples can be tested efficiently. Mechanosensing of endothelial cells activates Weibel–Palade bodies to secrete von Willebrand factor, a glycoprotein that mediates the adhesion of platelets. Endothelial cells tested in this device display shear regulation of von Willebrand factor, supporting the idea that mechanosensing is a necessary component of hemostasis and wound healing.

Fluidic shear stresses not only influences morphogenesis, but also migration behavior. Endothelial cell mechanotaxis under hemodynamic flow is an important function for wound healing and vascular repair. Cells at the edge of a wound increase their motility toward regions that are damaged, extending the leading edge and possibly modifying the ECM to allow other cells to proliferate and move in that direction. Microfluidic devices are used to investigate this behavior by applying a shear across monolayers of cells. Wounding assays are commonly done by dragging a sterile glass pipette or razor blade across a confluent layer of endothelial cells creating a fissure in the monolayer. By taking time-lapse images of the cells at the fissure, it is seen that cell migration is the dominant response in wound healing versus cell proliferation. Regardless of the wound direction, whether it is parallel or perpendicular to the fluid flow, shear stress increases wound closure rates. Migration rates through mechanotaxis have an impact on angiogenesis in developing organisms and vascular health and so the use of a bioreactor device aids in research understanding.[117] Other methods for creating wound simulation is to seed cells onto a surface with a thin film PDMS layer containing cut out areas. Cells grow to confluence and the film is removed exposing a patterned monolayer of cells.[118] The wound model demonstrates that cells at the leading edge of the wounded area sense the void and exhibit 'leader-cell' behavior, becoming highly mobile and acting to drag the cell layer into the missing region.

Microfluidics can be combined with other systems to better replicate *in vivo* conditions. Most commonly, factors or chemicals are added to media which is washed over cells. Combinations or gradients of factors can be created within devices to perform many experiments simultaneously.[119] Cell seeding density determines the number of cells in microchannels and can be changed to isolate single cells or create confluent monolayers. Force during the transmigration of leukocytes can be studied by combining fluid shear and endothelial cells on microposts. As cells such as neutrophils adhere during shear and pass through the endothelium, they impart forces to push the endothelial cells apart, which in experiments is detected by underlying micropost sensors.[120] Coculture of cells through the use of integrated three-dimensional ECM scaffolds in microfluidic devices can examine capillary growth, endothelial cell migration, and gradient growth factor effects.[121] For additional information, see **Chapter 5.512, *In Vivo* Bioreactors**.

3.315.5.5. Interstitial Shear

Mechanical shear is experienced by cells outside the vascular system as well. Interstitial flow is the slow movement of lymphatic fluid or blood plasma between ECM structures and cells. The fluid driving force is thought to be from difference in hydrostatic and osmotic pressures between the lymphatic system and vascular capillaries. The slow nature of the fluid flow is also explained by the presence of the proteoglycans fiber network that impedes the flow. Proteoglycans in the ECM are formed out of protein filaments with many glycosaminoglycan (GAG) side chain connections. These GAGs are able to bind to signal molecules or cytokines in the fluid by being negatively

charged. The physical geometry of the GAG side chains means that they present a densely packed but porous structure of overlapping strands. The combination of the hydrostatic or osmotic pressure differences and the flow resistance presented by the cell–ECM architecture work together to control the interchange rates of lymphatic fluid.

Interstitial flow is of interest due to its role in molecular transport within tissue and cells. In particular, tumors have been shown to have more permeable vasculature but a limited lymphatic path outward, causing them to tend to retain biomolecules. Specific micro- or nanoparticles can be designed to become concentrated in tumors and deliver therapeutic drugs.[122] Cell–ECM constructs or size controlled membranes are one route to simulate and examine interstitial flow on cultured cells while molecular fluorescent-labeling allows observation of the particles exchange rates. Integrated microfluidic systems that incorporate three-dimensional scaffolds and cell encapsulation can create interstitial flow effects by creating pressure differentials across different surfaces of the cell, maintaining a more native-like environment for examining phenomenon such as angiogenesis.[123]

3.315.5.6. Single Cell Analysis

In some cases, cell responses from a large population of cells can be misleading. One may observe that the expression levels of a particular protein is not centered on a point, but may have two distinct peak levels due to a bimodal behavior. Bulk measurements through immunoassays or gel electrophoresis techniques would suggest that the expression level is the average of the two peaks; however, this is flawed because it fails to resolve the two individual peaks. Probing individual cells is important to capture these phenomena.[124] BioMEMS cytometry tools exist such as fluorescent flow and laser scanning cytometry.[125] In fluorescent flow cytometry, cells in suspension have their specific biomolecules labeled with a fluorescent probe and are flowed past an illumination source and sensor. Concentration of the biomolecule on the surface of the cell is gathered through signal intensity and large numbers of cells can be screened this way. Laser scanning cytometry also uses fluorescent labeling, but individual cells in culture are positioned under the sensor for measurement. Advantages of this include being able to take time-lapse images of many cells in one experiment, and the cell does not need to be adherent. However, the process is slower than with flow cytometry.

BioMEMS techniques for physical trapping also exist, such as creating substrates with arrays of wells with room for cells. Cells are seeded into the wells, and nonadherent cells are washed away. This approach has been used to monitor the differentiation of mesenchymal stem cells that were exposed to different mixtures of adipogenic or osteogenic media conditions.[126] Confined growth channels have been applied to create micropatterns of muscle cells for long-term differentiation studies and fluorescent labeling.[127] Fluidic forces can be utilized like in hydrodynamic trap devices, which use small cross-flow channels to position cells within larger microchannels. Configurations have been used to examine cell–cell interactions by placing hydrodynamic traps across a channel to capture single cells and bring them in contact.[128] Microfluidic systems can also physically separate individual cells for analysis.[124] Examples include a novel design of microchannels that divert cells into cup-shaped wells. The hydrodynamics of a well with an occupied cell site prevents further cell occupation and allows for arrays of single cells to be analyzed (**Figure 16**). By creating channel systems with integrated valves, flow paths can be systemically changed to isolate out single cells for extraction of biomolecules such as messenger RNA[129] or by combining it with on-device electrophoresis, amino acid contents of single cells can be examined as well.[130]

3.315.5.7. Cell Sorting

Microfluidic sorting is possible with other BioMEMS tools. Antibody capture is one method that can select out target cells from a population because of cell surface chemistry changes upon differentiation. An antigen or antibody is applied to microstructures with high surface areas such as arrays of microposts or serpentine channels, and suspended cells are flowed across. Cell surface affinity for the antibody draws the cells to the structure while nontarget cells continue to pass (**Figure 15**). This is a robust technique that has been used to sort circulating prostate tumor cells from cell groups.[131]

As mentioned previously, optical traps have been used to stretch cells, but this technique can also be used to detect phenotypic difference between normal and cancerous cells and then sort the cells into different groups.[132] Cancerous cells have different cytoskeletal elastic and viscoelastic properties than normal cells. Research using normal 3T3 mouse fibroblast and malignant SV-T2 mouse fibroblasts under stretch has shown that optically induced deformations are statistically higher in the cancerous cells. Refractive index between the two cells is generally indistinguishable so similar optical stretch forces are exerted on both types. Cellular deformation then directly reflects the cytoskeletal deformation and compliance. Breast epithelial cells can also be distinguished despite a relatively low sampling count. Normal MCF10 breast epithelial cells have the least compliance, or are the stiffest. Cancerous MCF7 cells have more compliance and metastatic modMCF7 cells are the most compliant. This technique has a high throughput compared to previous techniques and a statistical conclusion can be reached rapidly. Phenotype sorting can be performed without potentially damaging physical or biochemical alteration to the cell populations such as with genomic techniques.

Optical sorting of dielectric particles and whole cells can be achieved by splitting a laser beam and focusing it to create interferometric patterns. These can be arranged into optical lattices of any dimension. Microchannel flow through these lattices generates a directional gradient that exerts different forces to alter the trajectory of the particle through a microchannel for sorting.[133] Optimization of the lattice focusing can give high sorting accuracy comparable with fluorescence sorting or flow cytometry techniques.

Integrating electrical fields on microfluidic systems can be done to use dielectrophoresis (DEP) for sorting and cell micromanipulation. A cell's membrane can act as a dielectric material and when an electrical field is applied, the field exerts a force on the cell in the direction of the strongest gradient. These forces can be used to trap cells in suspension for analysis using arrays of electrodes to generate standing electrical gradients.[134]

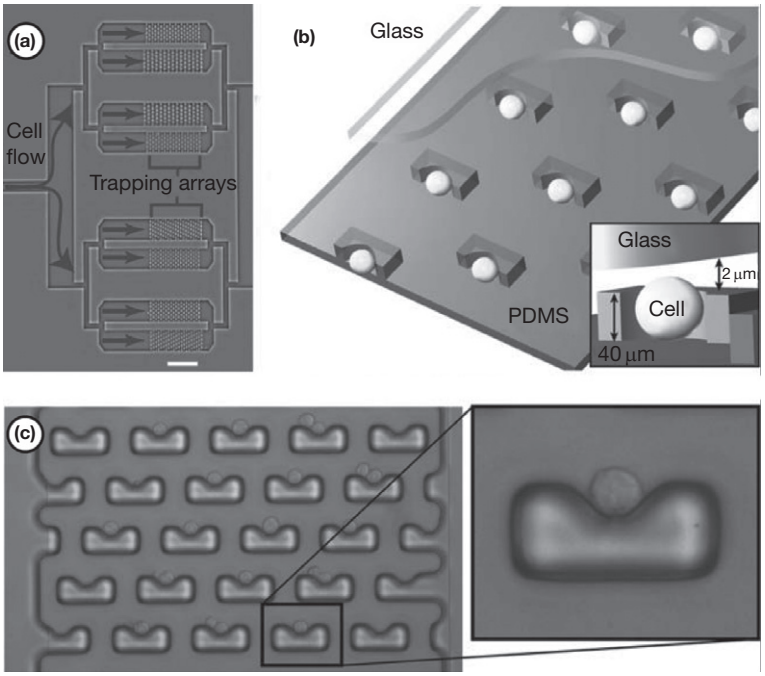

Figure 15 (a) Cell separation using (b) dimensioned heights and wells to (c) isolate single cells. Adapted from Di Carlo, D.D.; Wu, L.Y.; Lee, L.P.; *Lab Chip*, **2006**, *6*, 1445–1449, with permission from Royal Society of Chemistry.

The electrical properties of a cell's membrane can change depending on the proteins, biomolecules, or ions present in a cell during different differentiation states or cellular activities.[135] When a population of cells is exposed to electrical fields, DEP forces are exerted to differing degrees on the cells and allows for sorting them in a microfluidic system.[136]

3.315.5.8. Organ on Chip Microfluidic Devices

Research into the engineering of complete organ systems has benefited from microfluidic device studies as well. It has been possible to culture microtissue consisting of the heptatocytes in a fluidic bioreactor that supports cell viability and metabolic functionality of the liver.[137,138] Recently, a significant microfluidic system has been achieved that recreates the coculture cues and mechanical stimuli for cells of the pulmonary system.[139] The lung comprises individual alveolus which exchanges gas and chemicals with the blood. Similar to the endothelium, the alveolus are comprised of a single layer of alveolar epithelial cells with a meshwork of capillaries covering them. Gas and molecular exchange occurs through a thin ECM layer separating the epithelial cells and the endothelial cells of the capillaries as blood is pumped through the alveolus. There is also a strain effect induced as the alveolus fills with air during each respiratory cycle, with the elastic ECM aiding to expel the waste gas afterward. This is a complex system that is difficult to recreate with macroscale devices but has been achieved with a microfluidic system. First, a set of three parallel microchannels were constructed and bonded between a porous membrane (Figure 16(a)). The membrane is etched away in the left and right channels, but in the middle channel, it is partially etched so that a thin membrane separates the upper and lower

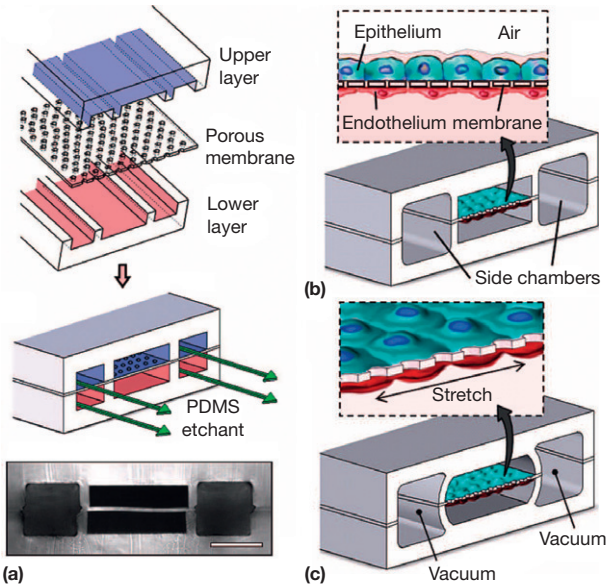

Figure 16 Lung-on-a-chip microdevice fabricated by (a) bonding two parallel PDMS microchannels around a PDMS membrane containing arrays of holes and etching steps. (b) Endothelial and epithelial cells can be grown on opposing sides of the membrane and exposed to shear and (c) stretch from applied vacuum. Adapted from Huh, D.; Matthews, B. D.; Mammoto, A.; Montoya-Zavala, M.; Hsin, H. Y.; Ingber, D. E. *Science* **2010**, *328*, 1662–1668.

channels. Alveolar epithelial cells can then be grown in the upper, center channel and pulmonary microvascular endothelial cells in the lower, center channel (Figure 16(b)). The left and right channels can be used to simulate strain from

respiratory cycling (Figure 16(c)). Researchers have used such devices to study coculture interactions between pulmonary cells and found that the barrier function of the alveolar epithelial cells and endothelial cells improved. Mechanical stretch used to mimic the motion of breathing accentuated the proinflammatory response to nanoparticles. These types of devices greatly improve the environmental cues seen by cells and can possibly replace animal testing by recreating whole-tissue physiology. For additional information, see **Chapter 3.309, Fluid Mechanics: Transport and Diffusion Analyses as Applied in Biomaterials Studies**.

3.315.5.9. Analysis of Mechanotransduction or Morphogenesis Biomarkers

In many BioMEMS applications and experiments, the presence or concentration of a protein is of interest to better understand the biochemical and biomechanical response of cells. To measure these, cell lysis is necessary to release intercellular contents of interest and can be performed through different BioMEMS techniques. Purely mechanical methods exist, such as forcing cells against micromachined barbs.[140] Another tool has been the development of micro system incorporated electroporation to disrupt the cell membrane without damaging organelle membranes.[141]

Immunofluoresence labeling is popular with researchers due to its target specificity. By using protein antibodies, single or multiple proteins to be examined together in one experimental sample to look at colocalization or compare expression levels. It is possible to perform the steps of immunostaining to cells inside a microfluidic device. To do so, the cells are washed with a fixative such as formalin or paraformaldehyde, whose aldehyde groups form methylene bridges between the nitrogen atoms of neighboring proteins. This treatment effectively cross-links the structure of the cell in place. The cell membrane is made permeable by adding a surfactant such as Triton X-100. Immunofluorescent staining utilizes a primary IgG antibody with affinity for specific antigens in a target protein of a cell. Blocking of nonspecific ligands in the cell can be accomplished by exposing samples to serum, which washes out unbound antibodies and serves to occupy nontargeted sites. A secondary antibody consisting of a fluorescent molecule conjugated to an IgG antibody to the primary antibody is then washed over the cell. The secondary antibody excites under a specific wavelength and emits photons at a higher wavelength. Single or multiple proteins can be placed on different excitation wavelengths to avoid signal interference. Because only targeted proteins or ligands are fluorescent, comparison between images for experimental and control samples gives researchers a method to cross-examine protein expression levels through signal intensity and an accurate way to identify protein colocalization sites. ELISA assays work under similar principles of antibody/antigen reactivity to detect presence or concentration in a sample. ELISA plates are scanned by a plate reader, and the intensity of the fluorescent signal indicates the amount of protein present in the sample. Microfluidic systems that perform ELISA on-chip have been used for disease detection and have an advantage over traditional assays by only requiring small amounts of biomarkers and reagents.[87]

In genomic techniques, microfluidics is a growing technology because of scaling advantages in biomolecular analysis.[142] In laboratory settings, amplification of DNA is traditionally done through polymerase chain reaction (PCR) techniques, but these generally require a sizeable sample from a population of at least 5000 cells, for which rare cells such as stem cells or circulating tumor cells may be difficult to obtain in large quantities. PCR and other amplification methodologies using BioMEMS can require as little as 150 cells, or only 300 pg. This technology and the level of sensitivity and detection have been demonstrated through human genome-wide transcriptome analysis.[143] Since external fluid handling is kept to a minimum, there is an improved sample accuracy in sensitive analyses such as PCR and electrophoresis.[144] In addition to mammalian cells, systems exist for the analysis of bacterial pathogens and viruses such as influenza.[145]

An interesting set of tools and assays are lab-on-disc or lab-on-CD technologies. These devices use microfluidic channels, gates, and switches imprinted into a spinning disc to perform many parallel evaluations of experimental samples. The microchannels are formed on a disc by photolithography and PDMS molding or injection molding plastics such as PMMA.[146] Force generated by spinning the device powers centrifugal pumping of fluid through the microchannels.[147] Different spin speeds cause the fluid to travel through channels that are gated by hydrophobic zones that act as burst valves. A fluid is able to move past a burst valve when the centrifugal force is large enough to overcome the surface tension of the fluid at the hydrophobic zone. Laser diode switchable gates can also be used to dynamically control the flow through the channels as the heat locally melts a barrier to the flow.[148] The design of the devices allows for processes such as mixing, metering, washing, reacting, and observation to occur in serial, entirely on disc, and is controlled by the spin speed profile.[149] Cell culture capabilities include growth and handling processes such as cell lysis.[150] ELISA assays have been converted to operate on discs and require less reagents and time than the standard large-scale assay.[151] Lab-on-disc is not limited to just fluids in the system but can also incorporate reagents bound on microbeads to increase surface area available for reactions. Immunoassays of whole blood in lab-on-disc have been performed to screen for diseases such as hepatitis and incorporate such protocols.[146] These microfluidic systems create a new opportunity to more completely investigate the spatial and temporal aspects of cell behavior by controlling the biochemical and biomechanical factors that a cell experiences and subsequently analyzing the response with integrated detection assays.

3.315.6. Future Directions

Many researchers are working toward better prosthetic integration with natural tissue. Currently, prosthetics are still largely perceived as foreign objects by the body. Few human-made materials can be accepted by living tissue on a cellular level and become incorporated with the native tissue. Through an understanding of migration, proliferation, differentiation, and adhesion that is aided by BioMEMS tools, future designs can better enhance biomaterial acceptance. This progress can be achieved by tailoring the material properties or soluble biochemistry to encourage migration through mechanotaxis or chemotaxis. BioMEMS tools also allow researchers to better control a cell's

microenvironment in order to elicit desirable behaviors from a cell. The development of new tools can offer better control of the biochemical and biomechanical environment properties or provide more powerful measurements. BioMEMS will continue to adapt from traditional MEMS application in order to improve. One such novel implementation has been the use of microfabricated nozzles for inkjet printers, which have been modified to deliver plasmids to targeted cells for gene transfection.[152] Microfluidics is particularly useful for engineering improvements for the cardiovascular system. For example, endothelial cell permeability from hemodynamic shear could be exploited for increased targeting of drugs to atherosclerotic lesions. Bioreactors could be used to culture megakaryocytes in order to generate large numbers of platelets to aid in blood transfusion. Surgical materials for stents can be biofunctionalized to prevent reocclusion of vessel walls after angioplasty, or can be constructed entirely of native ECM that can become fully incorporated into the tissue by encouraging cell motility and wound healing. Tools to impart microenvironment control for stem cells can enable better tissue engineering techniques in the future. These and many more examples demonstrate the potential for BioMEMS techniques and microenvironmental theories, which have merit for closer investigation.

Acknowledgments

The authors are grateful for support in part from grants from the National Institutes of Health (HL097284) and the National Science Foundation's CAREER Award.

References

1. Norman, J. J.; Mukundan, V.; Bernstein, D.; Pruitt, B. L. *Pediatr. Res.* **2008**, *63*, 576–583.
2. Sniadecki, N. J.; Desai, R. A.; Ruiz, S. A.; Chen, C. S. *Ann. Biomed. Eng.* **2006**, *34*, 59–74.
3. Geiger, B.; Spatz, J. P.; Bershadsky, A. D. *Nat. Rev. Mol. Cell Biol.* **2009**, *10*, 21–33.
4. Hahn, C.; Schwartz, M. A. *Nat. Rev. Mol. Cell Biol.* **2009**, *10*, 53–62.
5. Lo, C. M.; Wang, H. B.; Dembo, M.; Wang, Y. L. *Biophys. J.* **2000**, *79*, 144–152.
6. Thery, M.; Racine, V.; Pepin, A.; *et al. Nat. Cell Biol.* **2005**, *7*, 947–953.
7. Engler, A. J.; Sen, S.; Sweeney, H. L.; Discher, D. E. *Cell* **2006**, *126*, 677–689.
8. Mcbeath, R.; Pirone, D. M.; Nelson, C. M.; Bhadriraju, K.; Chen, C. S. *Dev. Cell* **2004**, *6*, 483–495.
9. Chen, C. S.; Mrksich, M.; Huang, S.; Whitesides, G. M.; Ingber, D. E. *Science* **1997**, *276*, 1425–1428.
10. Klein, E. A.; Yin, L.; Kothapalli, D.; *et al. Curr. Biol.* **2009**, *19*, 1511–1518.
11. Giancotti, F. G.; Ruoslahti, E. *Science* **1999**, *285*, 1028–1032.
12. Garcia, A. J.; Huber, F.; Boettiger, D. *J. Biol. Chem.* **1998**, *273*, 10988–10993.
13. Geiger, B.; Bershadsky, A.; Pankov, R.; Yamada, K. M. *Nat. Rev. Mol. Cell Biol.* **2001**, *2*, 793–805.
14. Burridge, K.; Wennerberg, K. *Cell* **2004**, *116*, 167–179.
15. Winder, S. J.; Ayscough, K. R. *J. Cell Sci.* **2005**, *118*, 651–654.
16. Bray, D. *Cell Movements: From Molecules to Motility*. Garland: New York, 2001.
17. Pellegrin, S.; Mellor, H. *J. Cell Sci.* **2007**, *120*, 3491–3499.
18. Zaidel-Bar, R.; Geiger, B. *J. Cell Sci.* **2010**, *123*, 1385–1388.
19. Ridley, A. J.; Hall, A. *Cell* **1992**, *70*, 389–399.
20. Ren, X. D.; Kiosses, W. B.; Sieg, D. J.; Otey, C. A.; Schlaepfer, D. D.; Schwartz, M. A. *J. Cell Sci.* **2000**, *113*(Pt 20), 3673–3678.
21. Lorenzo, A. C.; Caffarena, E. R. *J. Biomech.* **2005**, *38*, 1527–1533.
22. Ethier, C. R.; Simmons, C. A. *Introductory Biomechanics from Cells to Organisms*. Cambridge University Press: Cambridge, New York, 2007.
23. Suki, B.; Ito, S.; Stamenovic, D.; Lutchen, K. R.; Ingenito, E. P. *J. Appl. Physiol.* **2005**, *98*, 1892–1899.
24. Budynas, R. G.; Keith Nisbett, J. *Shigley's Mechanical Engineering Design*. McGraw-Hill: New York, 2008.
25. Vogel, V. *Annu. Rev. Biophys. Biomol. Struct.* **2006**, *35*, 459–488.
26. Vogel, V.; Sheetz, M. P. *Curr. Opin. Cell Biol.* **2009**, *21*, 38–46.
27. Pelham, R. J., Jr.; Wang, Y. *Proc. Natl. Acad. Sci. USA* **1997**, *94*, 13661–13665.
28. Jacot, J. G.; Mcculloch, A. D.; Omens, J. H. *Biophys. J.* **2008**, *95*, 3479–3487.
29. Cukierman, E.; Pankov, R.; Stevens, D. R.; Yamada, K. M. *Science* **2001**, *294*, 1708–1712.
30. Harris, A. K.; Wild, P.; Stopak, D. *Science* **1980**, *208*, 177–179.
31. Chrzanowska-Wodnicka, M.; Burridge, K. *J. Cell Biol.* **1996**, *133*, 1403–1415.
32. Helfman, D. M.; Levy, E. T.; Berthier, C.; *et al. Mol. Biol. Cell* **1999**, *10*, 3097–3112.
33. Burton, K.; Taylor, D. L. *Nature* **1997**, *385*, 450–454.
34. Harris, A. K.; Stopak, D.; Wild, P. *Nature* **1981**, *290*, 249–251.
35. Lee, J.; Leonard, M.; Oliver, T.; Ishihara, A.; Jacobson, K. *J. Cell Biol.* **1994**, *127*, 1957–1964.
36. Dembo, M.; Oliver, T.; Ishihara, A.; Jacobson, K. *Biophys. J.* **1996**, *70*, 2008–2022.
37. Dembo, M.; Wang, Y. L. *Biophys. J.* **1999**, *76*, 2307–2316.
38. Rajagopalan, P.; Marganski, W. A.; Brown, X. Q.; Wong, J. Y. *Biophys. J.* **2004**, *87*, 2818–2827.
39. Reinhart-King, C. A.; Dembo, M.; Hammer, D. A. *Mol. Biol. Cell* **2004**, *15*, 174a.
40. Munevar, S.; Wang, Y.; Dembo, M. *Biophys. J.* **2001**, *80*, 1744–1757.
41. Balaban, N. Q.; Schwarz, U. S.; Riveline, D.; *et al. Nat. Cell Biol.* **2001**, *3*, 466–472.
42. Shroff, S. G.; Saner, D. R.; Lal, R. *Am. J. Physiol. Cell Physiol.* **1995**, *38*, C286–C292.
43. Yuan, Y.; Verma, R. *Colloids Surf. B Biointerfaces* **2006**, *48*, 6–12.
44. Lal, R.; Drake, B.; Blumberg, D.; Saner, D. R.; Hansma, P. K.; Feinstein, S. C. *Am. J. Physiol. Cell Physiol.* **1995**, *38*, C275–C285.
45. Lal, R.; John, S. A. *Am. J. Physiol.* **1994**, *266*, C1.
46. Galbraith, C. G.; Sheetz, M. P. *Proc. Natl. Acad. Sci. USA* **1997**, *94*, 9114–9118.
47. Tan, J. L.; Tien, J.; Pirone, D. M.; Gray, D. S.; Bhadriraju, K.; Chen, C. S. *Proc. Natl. Acad. Sci. USA* **2003**, *100*, 1484–1489.
48. Zhou, J.; Ellis, A. V.; Voelcker, N. H. *Electrophoresis* **2010**, *31*, 2–16.
49. Mata, A.; Fleischman, A. J.; Roy, S. *Biomed. Microdevices* **2005**, *7*, 281–293.
50. Duffy, D. C.; McDonald, J. C.; Schueller, O. J. A.; Whitesides, G. M. *Anal. Chem.* **1998**, *70*, 4974–4984.
51. Tan, A.; Rodgers, K.; Murrihy, J.; O'Mathuna, C.; Glennon, J. D. *Lab Chip* **2001**, *1*, 7–9.
52. Slentz, B. E.; Penner, N. A.; Lugowska, E.; Regnier, F. *Electrophoresis* **2001**, *22*, 3736–3743.
53. Lemmon, C. A.; Sniadecki, N. J.; Ruiz, S. A.; Tan, J. L.; Romer, L. H.; Chen, C. S. *Mech. Chem. Biosyst.* **2005**, *2*, 1–16.
54. Sniadecki, N. J.; Lamb, C. M.; Liu, Y.; Chen, C. S.; Reich, D. H. *Rev. Sci. Instrum.* **2008**, *79*, 044302.
55. Addae-Mensah, K. A.; Kassebaum, N. J.; Bowers, M. J.; *et al. Sens. Actuators A Phys.* **2007**, *136*, 385–397.
56. Du Roure, O.; Saez, A.; Buguin, A.; *et al. Proc. Natl. Acad. Sci. USA* **2005**, *102*, 2390–2395.
57. Li, B.; Xie, L.; Starr, Z. C.; Yang, Z.; Lin, J. S.; Wang, J. H. *Cell Motil. Cytoskeleton* **2007**, *64*, 509–518.
58. Saez, A.; Buguin, A.; Silberzan, P.; Ladoux, B. *Biophys. J.* **2005**, *89*, L52–L54.
59. Saez, A.; Ghibaudo, M.; Buguin, A.; Silberzan, P.; Ladoux, B. *Proc. Natl. Acad. Sci. USA* **2007**, *104*, 8281–8286.
60. Kajzar, A.; Cesa, C. M.; Kirchgessner, N.; Hoffmann, B.; Merkel, R. *Biophys. J.* **2008**, *94*, 1854–1866.
61. Legant, W. R.; Pathak, A.; Yang, M. T.; Deshpande, V. S.; Mcmeeking, R. M.; Chen, C. S. *Proc. Natl. Acad. Sci. USA* **2009**, *106*, 10097–10102.
62. Liang, X. M.; Han, S. J.; Reems, J. A.; Gao, D.; Sniadecki, N. J. *Lab Chip* **2010**, *10*, 991–998.
63. Yang, M. T.; Sniadecki, N. J.; Chen, C. S. *Adv. Mater.* **2007**, *19*, 3119.
64. Nelson, C. M.; Jean, R. P.; Tan, J. L.; *et al. Proc. Natl. Acad. Sci. USA* **2005**, *102*, 11594–11599.
65. Liu, Z.; Tan, J. L.; Cohen, D. M.; *et al. Proc. Natl. Acad. Sci. USA* **2010**, *107*, 9944–9949.
66. Liu, Z. J.; Sniadecki, N. J.; Chen, C. S. *Cell. Mol. Bioeng.* **2010**, *3*, 50–59.
67. Fletcher, D. A.; Mullins, R. D. *Nature* **2010**, *463*, 485–492.
68. Mammoto, T.; Ingber, D. E. *Development* **2010**, *137*, 1407–1420.
69. Kaunas, R.; Nguyen, P.; Usami, S.; Chien, S. *Proc. Natl. Acad. Sci. USA* **2005**, *102*, 15895–15900.

70. Sawada, Y.; Sheetz, M. P. *J. Cell Biol*. **2002**, *156*, 609–615.
71. Giannone, G.; Sheetz, M. P. *Trends Cell Biol*. **2006**, *16*, 213–223.
72. Riveline, D.; Zamir, E.; Balaban, N. Q.; *et al*. *J. Cell Biol*. **2001**, *153*, 1175–1186.
73. Radmacher, M.; Tillmann, R. W.; Gaub, H. E. *Biophys. J*. **1993**, *64*, 735–742.
74. Yang, S.; Saif, T. *Rev. Sci. Instrum*. **2005**, *76*, 044301–044301-8.
75. Siechen, S.; Yang, S. Y.; Chiba, A.; Saif, T. *Proc. Natl. Acad. Sci. USA* **2009**, *106*, 12611–12616.
76. Wang, N.; Butler, J. P.; Ingber, D. E. *Science* **1993**, *260*, 1124–1127.
77. Matthews, B. D.; Overby, D. R.; Alenghat, F. J.; *et al*. *Biochem. Biophys. Res. Commun*. **2004**, *313*, 758–764.
78. Matthews, B. D.; Overby, D. R.; Mannix, R.; Ingber, D. E. *J. Cell Sci*. **2006**, *119*, 508–518.
79. Na, S.; Wang, N. *Sci. Signal*. **2008**, *1*, l1.
80. Hu, S.; Chen, J.; Fabry, B.; *et al*. *Am. J. Physiol. Cell Physiol*. **2003**, *285*, C1082–C1090.
81. Potard, U. S.; Butler, J. P.; Wang, N. *Am. J. Physiol*. **1997**, *272*, C1654–C1663.
82. Le Duc, Q.; Shi, Q.; Blonk, I.; *et al*. *J. Cell Biol*. **2010**, *189*, 1107–1115.
83. Chen, C. S.; Tan, J.; Tien, J. *Annu. Rev. Biomed. Eng*. **2004**, *6*, 275–302.
84. Choquet, D.; Felsenfeld, D. P.; Sheetz, M. P. *Cell* **1997**, *88*, 39–48.
85. Galbraith, C. G.; Yamada, K. M.; Sheetz, M. P. *J. Cell Biol*. **2002**, *159*, 695–705.
86. Jiang, G.; Giannone, G.; Critchley, D. R.; Fukumoto, E.; Sheetz, M. P. *Nature* **2003**, *424*, 334–337.
87. Wang, Y.; Botvinick, E. L.; Zhao, Y.; *et al*. *Nature* **2005**, *434*, 1040–1045.
88. Nambiar, R.; McConnell, R. E.; Tyska, M. J. *Proc. Natl. Acad. Sci. USA* **2009**, *106*, 11972–11977.
89. Guck, J.; Ananthakrishnan, R.; Moon, T. J.; Cunningham, C. C.; Kas, J. *Phys. Rev. Lett*. **2000**, *84*, 5451–5454.
90. Meiners, J. C.; Quake, S. R. *Phys. Rev. Lett*. **2000**, *84*, 5014–5017.
91. Moffitt, J. R.; Chemla, Y. R.; Izhaky, D.; Bustamante, C. *Proc. Natl. Acad. Sci. USA* **2006**, *103*, 9006–9011.
92. Finer, J. T.; Simmons, R. M.; Spudich, J. A. *Nature* **1994**, *368*, 113–119.
93. Arsenault, M. E.; Sun, Y.; Bau, H. H.; Goldman, Y. E. *Phys. Chem. Chem. Phys*. **2009**, *11*, 4834–4839.
94. Beausang, J. F.; Schroeder, H. W., III; Nelson, P. C.; Goldman, Y. E. *Biophys. J*. **2008**, *95*, 5820–5831.
95. Sniadecki, N. J.; Anguelouch, A.; Yang, M. T.; *et al*. *Proc. Natl. Acad. Sci. USA* **2007**, *104*, 14553–14558.
96. Trepat, X.; Deng, L.; An, S. S.; *et al*. *Nature* **2007**, *447*, 592–595.
97. Krishnan, R.; Park, C. Y.; Lin, Y. C.; *et al*. *PLoS One* **2009**, *4*, e5486.
98. Colombelli, J.; Besser, A.; Kress, H.; *et al*. *J. Cell Sci*. **2009**, *122*, 1665–1679.
99. Kumar, S.; Maxwell, I. Z.; Heisterkamp, A.; *et al*. *Biophys. J*. **2006**, *90*, 3762–3773.
100. El-Ali, J.; Sorger, P. K.; Jensen, K. F. *Nature* **2006**, *442*, 403–411.
101. Masters, J. R.; Stacey, G. N. *Nat. Protoc*. **2007**, *2*, 2276–2284.
102. Malek, A. M.; Alper, S. L.; Izumo, S. *J. Am. Med. Assoc*. **1999**, *282*, 2035–2042.
103. Cunningham, K. S.; Gotlieb, A. I. *Lab. Invest*. **2005**, *85*, 9–23.
104. Garcia-Cardena, G.; Comander, J.; Anderson, K. R.; Blackman, B. R.; Gimbrone, M. A., Jr. *Proc. Natl. Acad. Sci. USA* **2001**, *98*, 4478–4485.
105. Dai, G.; Kaazempur-Mofrad, M. R.; Natarajan, S.; *et al*. *Proc. Natl. Acad. Sci. USA* **2004**, *101*, 14871–14876.
106. Steward, R. L., Jr.; Cheng, C. M.; Wang, D. L.; Leduc, P. R. *Cell Biochem. Biophys*. **2010**, *56*, 115–124.
107. Barbee, K. A.; Davies, P. F.; Lal, R. *Circ. Res*. **1994**, *74*, 163–171.
108. Nesbitt, W. S.; Westein, E.; Tovar-Lopez, F. J.; *et al*. *Nat. Med*. **2009**, *15*, 665–673.
109. Rubenstein, D. A.; Yin, W. *J. Thromb. Thrombolysis* **2010**, *30*, 36–45.
110. Junt, T.; Schulze, H.; Chen, Z.; *et al*. *Science* **2007**, *317*, 1767–1770.
111. Reneman, R. S.; Arts, T.; Hoeks, A. P. *J. Vasc. Res*. **2006**, *43*, 251–269.
112. Santiago, J. G.; Wereley, S. T.; Meinhart, C. D.; Beebe, D. J.; Adrian, R. J. *Exp. Fluids* **1998**, *25*, 316–319.
113. Wallace, C. S.; Champion, J. C.; Truskey, G. A. *Ann. Biomed. Eng*. **2007**, *35*, 375–386.
114. Frangos, J. A.; Eskin, S. G.; Mcintire, L. V.; Ives, C. L. *Science* **1985**, *227*, 1477–1479.
115. Chiu, J. J.; Wang, D. L.; Chien, S.; Skalak, R.; Usami, S. *J. Biomech. Eng*. **1998**, *120*, 2–8.
116. Chau, L.; Doran, M.; Cooper-White, J. *Lab Chip* **2009**, *9*, 1897–1902.
117. Li, S.; Huang, N. F.; Hsu, S. *J. Cell Biochem*. **2005**, *96*, 1110–1126.
118. Poujade, M.; Grasland-Mongrain, E.; Hertzog, A.; *et al*. *Proc. Natl. Acad. Sci. USA* **2007**, *104*, 15988–15993.
119. Neils, C.; Tyree, Z.; Finlayson, B.; Folch, A. *Lab Chip* **2004**, *4*, 342–350.
120. Rabodzey, A.; Alcaide, P.; Luscinskas, F. W.; Ladoux, B. *Biophys. J*. **2008**, *95*, 1428–1438.
121. Chung, S.; Sudo, R.; Mack, P. J.; Wan, C. R.; Vickerman, V.; Kamm, R. D. *Lab Chip* **2009**, *9*, 269–275.
122. Swartz, M. A.; Fleury, M. E. *Annu. Rev. Biomed. Eng*. **2007**, *9*, 229–256.
123. Vickerman, V.; Blundo, J.; Chung, S.; Kamm, R. *Lab Chip* **2008**, *8*, 1468–1477.
124. Di Carlo, D.; Lee, L. P. *Anal. Chem*. **2006**, *78*, 7918–7925.
125. Mach, W. J.; Thimmesch, A. R.; Orr, J. A.; Slusser, J. G.; Pierce, J. D. *J. Clin. Monit. Comput*. **2010**, *24*(4), 251–259.
126. Gomez-Sjoberg, R.; Leyrat, A. A.; Pirone, D. M.; Chen, C. S.; Quake, S. R. *Anal. Chem*. **2007**, *79*, 8557–8563.
127. Tourovskaia, A.; Figueroa-Masot, X.; Folch, A. *Lab Chip* **2005**, *5*, 14–19.
128. Lee, P. J.; Hung, P. J.; Shaw, R.; Jan, L.; Lee, L. P. *Appl. Phys. Lett*. **2005**, *86*, 223902–223902-3.
129. Hong, J. W.; Studer, V.; Hang, G.; Anderson, W. F.; Quake, S. R. *Nat. Biotechnol*. **2004**, *22*, 435–439.
130. Wu, H.; Wheeler, A.; Zare, R. N. *Proc. Natl. Acad. Sci. USA* **2004**, *101*, 12809–12813.
131. Stott, S. L.; Lee, R. J.; Nagrath, S.; *et al*. *Sci. Transl. Med*. **2010**, *2*, 25ra23.
132. Guck, J.; Schinkinger, S.; Lincoln, B.; *et al*. *Biophys. J*. **2005**, *88*, 3689–3698.
133. MacDonald, M. P.; Spalding, G. C.; Dholakia, K. *Nature* **2003**, *426*, 421–424.
134. Voldman, J.; Gray, M. L.; Toner, M.; Schmidt, M. A. *Anal. Chem*. **2002**, *74*, 3984–3990.
135. Hu, X.; Arnold, W. M.; Zimmermann, U. *Biochim. Biophys. Acta* **1990**, *1021*, 191–200.
136. Gascoyne, P. R.; Vykoukal, J. V. *Proc. IEEE Inst. Electr. Electron. Eng*. **2004**, *92*, 22–42.
137. Powers, M. J.; Domansky, K.; Kaazempur-Mofrad, M. R.; *et al*. *Biotechnol. Bioeng*. **2002**, *78*, 257–269.
138. Powers, M. J.; Janigian, D. M.; Wack, K. E.; Baker, C. S.; Beer Stolz, D.; Griffith, L. G. *Tissue Eng*. **2002**, *8*, 499–513.
139. Huh, D.; Matthews, B. D.; Mammoto, A.; Montoya-Zavala, M.; Hsin, H. Y.; Ingber, D. E. *Science* **2010**, *328*, 1662–1668.
140. Di Carlo, D.; Jeong, K. H.; Lee, L. P. *Lab Chip* **2003**, *3*, 287–291.
141. Lu, H.; Schmidt, M. A.; Jensen, K. F. *Lab Chip* **2005**, *5*, 23–29.
142. Zhang, C.; Xu, J.; Ma, W.; Zheng, W. *Biotechnol. Adv*. **2006**, *24*, 243–284.
143. Irimia, D.; Mindrinos, M.; Russom, A.; *et al*. *Integr. Biol. (Camb.)* **2009**, *1*, 99–107.
144. Lagally, E. T.; Medintz, I.; Mathies, R. A. *Anal. Chem*. **2001**, *73*, 565–570.
145. Pal, R.; Yang, M.; Lin, R.; *et al*. *Lab Chip* **2005**, *5*, 1024–1032.
146. Lee, B. S.; Lee, J. N.; Park, J. M.; *et al*. *Lab Chip* **2009**, *9*, 1548–1555.
147. Madou, M.; Zoval, J.; Jia, G. Y.; Kido, H.; Kim, J.; Kim, N. *Annu. Rev. Biomed. Eng*. **2006**, *8*, 601–628.
148. Park, J. M.; Cho, Y. K.; Lee, B. S.; Lee, J. G.; Ko, C. *Lab Chip* **2007**, *7*, 557–564.
149. Duffy, D. C.; Gillis, H. L.; Lin, J.; Sheppard, N. F.; Kellogg, G. J. *Anal. Chem*. **1999**, *71*, 4669–4678.
150. Kim, J.; Hee Jang, S.; Jia, G.; Zoval, J. V.; da Silva, N. A.; Madou, M. J. *Lab Chip* **2004**, *4*, 516–522.
151. Lai, S.; Wang, S.; Luo, J.; Lee, L. J.; Yang, S. T.; Madou, M. J. *Anal. Chem*. **2004**, *76*, 1832–1837.
152. Xu, T.; Rohozinski, J.; Zhao, W.; Moorefield, E. C.; Atala, A.; Yoo, J. J. *Tissue Eng. A* **2009**, *15*, 95–101.